MONTE CARLO SIMULATIONS OF METHANOL ABSORPTION AND CLUSTERING IN POLYVINYLCHLORIDE AND HIGH DENSITY POLYETHYLENE

Shresta Ganesh

In fulfilment of the Degree of Master of Engineering in Chemical Engineering, Faculty of Engineering and the Built Environment, Durban University of Technology

December 2016

Supervisor: Mr. S. Ramsuroop

Co-supervisor: Dr. M. Lasich

As the candidate's supervisors, we agree to the submission of this thesis.

_____ _____

Mr. S. Ramsuroop **Dr. M. Lasich**

I, Shresta Ganesh, declare that:

(I) The research reported in this dissertation/thesis, except where otherwise indicated, is my original work.

(II) This dissertation/thesis has not been submitted for any degree or examination at any other university.

(III) This dissertation/thesis does not contain other persons' data, pictures or graphs or other information, unless specifically acknowledged as being sourced from other persons.

(IV) This dissertation/thesis does not contain other persons' writing, unless specifically acknowledged as being sourced from other researchers. Where other sources have been quoted, then:

a) Their words have been re-written but the general information attributed to them has been referenced:

b) Where their exact words have been used, their writing has been placed inside quotation marks and referenced.

(V) Where I have reproduced a publication of which I am an author, co-author or editor, I have indicated in detail which part of the publication was actually written by myself alone and have fully referenced such publications.

(VI) This dissertation/thesis does not contain text, graphics or tables copied and pasted from the internet, unless specifically acknowledged, and the source being detailed in the dissertation/thesis and in the References sections.

_____

S. Ganesh

ACKNOWLEDGEMENTS

I would like to acknowledge and thank the following individuals and organisations for their role in my educational journey:

My supervisors, Dr M Lasich and Mr S Ramsuroop, for overseeing the work required for this thesis. In particular, I would like to express my sincere gratitude to Dr Lasich, whose guidance, advice and help throughout my academic career has been invaluable. I wish to thank him for all his efforts in assisting me in seeing this thesis to completion. It was the steadfast support and interest in my progress from Dr Lasich that has allowed me to persevere in the academics of engineering. I am very grateful for this learning experience which has opened the doors to my becoming a researcher due to interactions with Dr Lasich.

I would like to thank the Centre for High Performance Computing (CHPC) for the use of their systems in running simulations.

I would like to thank my uncle, Raynund Ganesh, for his unconditional support, help and advice regarding my studies and career.

I dedicate this thesis to my mother, Sandhia Randhir Panchoo, for always endeavouring to ensure my education despite the difficult circumstances. Thank you for all that you do.

To my guiding Gods, Saraswati Mata and Lord Shiva, thank you for blessing me so abundantly in life and providing me with true education.

ABSTRACT

A pertinent issue facing the materials industry is that of the lifespan of materials when exposed to certain solvents/ environments. Limitations to the applications of materials require further research into understanding their failure mechanisms and how such problems can be addressed in terms of re-engineering such materials to be more durable. PVC and HDPE are two common polymers used extensively in industrial applications. Gibbs ensemble Monte Carlo simulations were used to simulate systems of PVC and HDPE with methanol, respectively. The temperatures used in this work were 25, 30 and 40 ^{o}C and all systems were at atmospheric pressure. Laboratory tests were used to complement simulations for analysis purposes. Results showed an increase in temperature resulted in a decrease in the overall clustering in both polymers although PVC displayed a greater decrease than HDPE. Linear clustering dominated over other forms of clustering with increases in temperature, with dimers being the most prevalent topology type. The results of this study suggest that the presence of chlorine atoms in PVC may not directly affect clustering of absorbed methanol, and their effect may instead be indirect by means of altering the accessible free volume within the polymer. Swelling was also investigated in the simulated systems and it was found that PVC displayed a greater degree of swelling than HDPE despite its lower rate of clustering. The effect of cluster radius on the cluster analysis was also considered.

TABLE OF CONTENTS

Page No.

LIST OF TABLES

Note: The tables in the appendices are not included in this list.

LIST OF FIGURES

NOMENCLATURE

Symbols:

Å	Angstroms
D	Bond association energy
E	Total potential energy
j	microstate
k_B	Boltzmann Constant
k_{ij}	Force Constant
n	Energy level
N	Number of molecules in a system
p	Probability
P	Pressure
r	Intermolecular/interatomic distance
T	Temperature
U	Internal energy
V	Volume
W	Unique states
z	Activity Coefficient

Greek Symbols:

ε	Lennard-Jones parameter describing the potential well depth
λ	de Broglie wavelength of constituent particles
μ	Chemical potential
π	The ratio of a circle's circumference to its diameter
$\sum$	Denotes the summation of the elements of a series or set
σ	Lennard-Jones parameter describing the distance at which the potential function equals zero
Ω	Number of microstates

Subscripts:

$_{el}$	Associated with electrostatic terms
$_{i,j}$	Describes interactions between i^{th} and j^{th} elements
$_{R}$	Associated with bond stretching
$_{vdw}$	Associated with van Der Waals terms
$_{\omega}$	Associated with inversion terms
$_{\theta}$	Associated with bond angle bending
$_{\phi}$	Associated with dihedral angle torsion

CHAPTER 1: INTRODUCTION

"Who never walks save where he sees men's tracks makes no discoveries." __ J.G Holland

Polymers have an array of industrial applications ranging from piping to storage tanks yet a pressing scientific issue facing industries is their failure when exposed to industrial solvents which may be due to weakening of the polymer structure over long time periods. The study of material science and engineering can aid in better understanding the fundamental behaviour of such widely used or common products hence it is highly beneficial to gain more insight into the equilibrium behaviour of polymers in contact with solvents, both from an industrial viewpoint and in terms of basic research. The work described herein concerns the interactions of methanol, a common industrial alcohol, with polyvinylchloride (PVC) and high density polyethylene (HDPE), two widely used polymers. The importance of analysing alcohol molecules within the matrix of polymers stems from the work of Johansson (2007) who studied the clustering of water molecules in polyethylene. The findings of this study on the water and polyethylene system showed that the degradation of the polymer matrix was related to the clustering of water molecules around charged ions. Therefore, knowledge of the capabilities or the likelihood of alcohol molecules forming large (typically cyclic) clusters can assist with understanding the mechanisms behind the degradation of synthetic polymers exposed to alcohol solutions.

Until recently, new materials were found by trial and error processes which can be tedious and time consuming. With the increase in computing power and major advances in the technology associated with scientific computing, simulating the behaviour of materials has become possible. A shortfall of laboratory experiments is that certain conditions are physically unattainable. Molecular modelling and simulation overcomes these physical limitations and can provide insights that would otherwise be impossible to obtain via physical experimentation on a macroscopic scale. This study employed the Monte Carlo simulation scheme of Metropolis et al (1953) to study systems of PVC or HDPE and methanol. This research aimed at determining the temperature dependence of methanol absorption and clustering in PVC and HDPE, ultimately investigating how the polymers influence the

clustering of alcohols, methanol in particular at atmospheric pressure and temperatures of 25, 30 and 40 ^{o}C. These temperatures were chosen so as to remain close to realistic industrial conditions.

The objectives of this study included the following:

- Conduct experimental measurements of methanol absorption in PVC and HDPE at 3 different temperatures and ambient pressure.
- Simulate absorption at the same conditions for qualitative and quantitative verification of molecular force fields
- Performing cluster analysis of spatial coordinates resulting from the simulations.
- Establishing the absorption mechanisms of alcohols in PVC and HDPE

The Monte Carlo method is a statistical approach involving several different techniques that extensively employ the use of random numbers to create changes in the system that may be accepted or rejected according to changes of the system's potential energy. This method, independent of time, creates configurations that would be possible and probable if the system were at equilibrium. Due to the potentially infinite number of possible configurations that are generated from simulations, a single Monte Carlo configuration cannot be used to ascertain any conclusions. Therefore, millions of configurations are generated and the parameters and properties of interest are obtained by taking an average of the generated configurations. Monte Carlo simulation is therefore a suitable method for dealing with systems at equilibrium.

CHAPTER 2: LITERATURE REVIEW

"To do successful research, you don't need to know everything; you just need to know of one thing that isn't known." __ Arthur Schawlow

2.1 The Beginning of the Monte Carlo Method

The development of the Monte Carlo method, at least the form implemented in this study, parallels that of the development of the first electronic computer, Electronic Numerical Integrator And Computer (ENIAC) during the 1940's. During this time of intensive work on the ENIAC, physicists and engineers became aware that if electronic circuits could count then arithmetic computations would be possible thus solving, inter alia, differential equations at unthinkable speeds. During the review of the ENIAC's processing ability, Stan Ulam, an active mathematician at the time, with an interest in random processes realised that statistical sampling techniques, which up to that point were not pursued due to the tediousness and length of their calculations, could now be undertaken with relative ease which ultimately led to the Monte Carlo method for molecular simulations (Metropolis 1987: 125-130).

2.2 The Monte Carlo Method

The Monte Carlo method is a statistical sampling technique which uses random sampling to estimate mathematical functions and mimic the behaviour of a variety of complex systems. It should be noted that simulations do not give exact solutions as they are only as good as the accuracy of the models and inputs used, however, they can be used to obtain insight into systems that cannot be well visualised by an experimental method. Simulations are thus complementary to analytical and experimental studies. All Monte Carlo simulations have a general method of approach which is outlined as follows:

- Model a system as a (series of) probability distribution functions (PDF's)
- Take an initial configuration *i* and propose a change to a new configuration *j*
- Accept the new configuration with probability of that less than the old configuration
- Measure the quantities of interest
- Repeatedly sample from the PDF's

- Tally/ compute the statistics of interest

The method involves initially defining a model that is able to express the behaviour of a system fairly closely to that of a realistic system.

Using this random sampling a Markov chain is constructed such that it has the desired distribution as the equilibrium distribution, where a Markov chain is stochastic process that is described "memory-less". In other words the probability distribution of the subsequent state is only dependent on the current state and not on how the current state was achieved. The Markov chain is constructed until convergence is achieved.

2.3 Molecular Theory

Molecules by their very nature are small and light with common linear dimensions having magnitudes between 10^{-10} to 10^{-8} m and masses between 10^{-27} and 10^{-25} kg (Smith, Van Ness and Abbott (2005)). From this, it is clear that the number of molecules in a macroscopic system is extremely large. Such features of miniscule mass, smallness and large numbers of interacting particles require the use of quantum and statistical mechanics to describe the behaviour of the system at a molecular level and to extrapolate this to a macroscopic scale.

A two – step approach is required for the study of physical properties via molecular theory. These involve calculating the energy of the system and then solving statistical mechanics equations pertaining to a system with such a potential (Gubbins (1993)) where the desired solution is to obtain a state with that corresponding to the lowest energy/ free energy. The total energy of a system comprises of the sum of the intermolecular and intramolecular energies.

2.4 Simulation Techniques

Two common approaches can be used to simulate systems of atoms or molecules. These simulation methods can be broadly classified into molecular dynamics (MD) and the Monte Carlo (MC) approach. Molecular dynamics, which is based on the classical mechanical description of molecular motion, follows a system's trajectory through phase space via the integration of Newton's equations of motion. With this method, thermodynamic properties of molecular systems can be calculated with respect to time and therefore molecular dynamics is suitable for studying time-dependent properties. Molecular dynamics has been used in various studies to examine the mechanism of diffusion through polymer membranes as seen

in the works of Tamai (1994) and Pant and Boyd (1993). As mentioned previously, the Monte Carlo approach determines the average value of the properties of a system for a number of acceptable configurations rather than considering the behaviour of the system overtime. The Monte Carlo scheme randomly applies random moves to molecules thus mimicking molecular behaviour. The probability of accepting each change is dependent on the energy difference between the initial and final configuration. Moves are rejected for energy changes above a predetermined tolerance thus a statistical average across different states can be computed. This can overcome the issue of the time taken to reach equilibrium in a molecular dynamics simulation which can be computationally expensive. This method has been extensively used in research relating to clustering of molecules as can be seen from the works of Johansson (2007) and Lasich (2011).

2.5 Previous Work

Investigations conducted by Johansson et al (2007) considered the clustering of water molecules in polyethylene. Due to the strong polarity of water molecules, clustering can occur as each molecule has a distinct negative and positive Coulombic charge. Hydrogen atoms are positively charged while oxygen atoms possess a negative charge. Such localised charges are highly influential in their contribution to what geometric arrangements water molecules may take when in contact with each other. The geometric arrangements can be defined by their topologies and are known as clusters. Various topological forms exist such as branched, cyclic or linear and may be composed of different numbers of water molecules. Their findings showed the degradation of the polymer matrix over long periods of time was related to water molecules clustering around charged ions. Their significant conclusion was that impurity ions which entered the polymer matrix during extrusion processes resulted in the attraction of water molecules around the ions. The water molecules were successful in penetrating and forming large, non-linear clusters in the polymer matrix which ultimately explains the failure mechanism of the material when exposed to humidity or liquid water.

Lasich, Johansson and Ramjugernath (2011) investigated the solubility of water molecules in polytetrafluroethylene (PTFE). Their aim was to determine the influence of temperature, if at all, and perfluoroalkane chain length on the solubility of water in the perfluoroalkane phase. Their work using PTFE was built on from studies conducted by Johansson (2007), who used polyethylene, which served as a basis of comparison. They concluded that overall there was

significantly higher solubility of water into polytetrafluoroethylene / perfluoroalkanes than was observed in polyethylene/alkanes.

This study on water and polytetrafluoroethylene / perfluoroalkanes was extended into investigating the clustering of water molecules in polytetrafluorotheylene (Lasich, Johansson and Ramjugernath (2013)) by varying the carbon number in the polymer chain and temperature. The Monte Carlo approach with the Gibbs ensemble was used to simulate these systems. Their main finding was that an increase in temperature resulted in an increase in the number of water molecules found in all clusters. However, for polymer chain lengths of 50 carbon atoms they found an apparent decrease in the fraction of water molecules found in clusters. They attributed this to the fact that at large carbon numbers there exists a large free volume within the polymer matrix into which water molecules may move freely. This free space does not readily lend itself to clustering of water molecules as the free space allows for more dispersed aggregations of water molecules.

Simulations of water clusters in vapour, alkanes and polyethylene were conducted by Bolton et al (2009). This was one of the first molecular level investigations where all four critical components (as far as the present study is concerned) i.e. water, polyethylene, electric field and ionic impurities were included in order to critically examine water treeing. Water treeing is the formation of tree-like branching defects within the polyethylene due to the action of water or humidity, which ultimately leads to the degradation of, in the case of the aforementioned study, the polyethylene insulation surrounding electrical cables. Their aim was to determine the effects of the above mentioned components on the formation of water clusters and how such clusters lead to water treeing in polyethylene cables. The Gibbs Ensemble Monte Carlo (GEMC) technique was used combined with an electric field. The simulations included a Na^+ - Cl^- ion pair in the hydrocarbon matrix and external electric fields were simulated enabling the effect of enhancing or weakening the local field to be investigated. It was found that the presence of the ion pairs leads to a significant increase in the solubility of water in polyethylene. They claimed that rod-like structures are formed by water molecules between ion pairs when they are close enough. For ion pairs far apart (25 Å), it was found that rod-like structures were not well supported due to a poor local electric field and instead water clusters formed around each ion. This led to a decrease in the solubility of water. They also concluded that the presence of an electric field enhances the local field between the ions resulting in an increase in water up-take. From these findings, they were

able to hypothesise a possible mechanism for water tree formation in electric cable insulation made from polyethylene.

Pal et al (2005) used molecular dynamics simulations to examine the hydrophobicity of nanostructured alkane and perfluoroalkane surfaces. The results showed that the water molecules interacted very little with the surface of the perfluorinated alkane and did not penetrate the crystal body. This suggests that a simple correction can be applied to the results of simulations performed using purely amorphous polymers, in terms of the amount of a penetrant species absorbed into the polymer matrix.

In an attempt at predicting phase equilibria via molecular simulation; Fuchs, Boutin and Rousseau (1998), considered a mixture of methane and n-pentane which they simulated using the Gibbs Ensemble technique. The anisotropic united atom (AUA) and united atom (UA) models of Smit, Karaborni and Siepmann (1995) were used and results of phase behaviour were compared to experimental values. It was found that both models rendered reasonable quantitative predictions for liquid and vapour phase densities in contrast to experimental values, with a small overestimation of the liquid density by the UA model. An agreement between composition predictions of model and experimental values for the liquid phase was observed and the AUA model agreed well with the vapour phase composition.

Mingxue, Wenchuan and Huanzhang (1992), used the Gibbs Ensemble Monte Carlo method to study vapour-liquid equilibria of a real binary mixture of argon and methane. This study was done to obtain micro-structural and microscopic properties, distribution function, internal energy, densities, compositions and enthalpy of vapourization of the co-existing phases. This data was validated using experimental measurements as well as results calculated from equations of state. Their results showed that the uncertainties of compositions were miniscule and in agreement with the experimental data. The enthalpies for the vapour and liquid phases obtained from the simulations proved satisfactory when compared with estimations obtained from equations of state. Their primary conclusion was that the Gibbs method is a powerful tool in research regarding phase equilibria of fluids and can be applied to more complex, real mixtures.

The application of Monte Carlo methods to calculate transport diffusion coefficients for hydrogen and hydrocarbons in carbon membranes containing nanopores was accomplished by Seo, Kum and Seaton (2001). Surface diffusion was used to characterise molecular movements where strong fluxes were achieved close to the pore wall. They established that

pore size presented as a significant factor in determining the selectivity of hydrocarbons within the membrane. There was a semi-quantitative agreement between their calculated diffusivities and that of published experimental data.

In a similar study but employing the use of molecular dynamics, Li et al (1997) examined the diffusion of small molecules in four different amorphous polymers. Calculated diffusion coefficients were compared to values obtained experimentally. It was found that there was a good correlation between calculated and experimental values when dealing with systems of hydrophobic molecules diffusing through hydrophobic polymers. It was seen that for small molecules, the diffusion process was affected by water molecules that diffuse into the polymer occupying free spaces. Their study ultimately concluded that computer simulated molecular diffusion is more useful in obtaining relative values rather than absolute diffusion coefficient values.

A more current study by Börjesson et al (2013) concerning oxygen and water permeation in polyethylene used both Monte Carlo and molecular dynamics simulations to obtain diffusion, solubility and permeation coefficients for the respective permeants in polyethylene in order to obtain a molecular level understanding of the diffusion mechanism. They established that the penetrants diffuse through the polymer via large amplitude, infrequent jumps where the average size of the water jumps was smaller than that of oxygen. Furthermore, diffusion coefficients of oxygen and water were forced to have similar magnitudes and increased with an increase in temperature although the increase was larger for water than for oxygen. They attributed this to the larger activation barrier for diffusion of water through polyethylene. Solubility and permeation coefficients for oxygen were orders of magnitude higher than that of water. Due to the wide availability of experimental data, a comparison between experimental and simulated data was not feasible; however, the qualitative and semi-quantitative trends between both types of data were in agreement.

Adsorption isotherms of pure and a binary mixture of water and furfural in polyurethane membranes were investigated by Rahmati, Modarress and Gooya (2012) using the configurational bias - grand canonical Monte Carlo (CB – GCMC) simulation technique. This was to observe the effect on adsorption and separation properties on membranes made from polyurethane, of the degree of polymerization in a temperature range of 298 to 360 K and 0 to 10 bar pressure. It was found that an increase in the degree of polymerization caused polyurethane chains to fold and start rotating around themselves thus affecting the physical

and separation properties of the polyurethane membrane. They also observed an increase in the adsorption of furfural and water. For this study, the researchers also investigated the structural and physical properties of polyurethane membranes and the effect of the degree of polymerization on these properties by the use of molecular dynamics simulations. Results were compared to experimental data and a good agreement was observed.

2.6 Previous Experiments

Experiments conducted by Freire et al (2009) investigated the solubility of water in fluoro- and perfluorocarbons. They used a temperature range of 288.15 K to 318.15K. They found the solubility of water in perfluorocarbons, as expressed in terms of the mole fractions, to be strongly dependent on temperature. They also found the solubility to increase significantly from cyclic perfluorocarbons to n-perfluoroalkanes to aromatic perfluorocarbons. They suggested this is due to the interaction of water with the perfluorocarbon π - system which results from the decrease in the π electron density of the perfluorinated aromatic ring.

T/K	C_7F_{14} 10^4 $(x \pm \sigma^a)$	$C_{10}F_{18}$ 10^4 $(x \pm \sigma^a)$	C_6F_6 10^3 $(x \pm \sigma^a)$	C_7F_8 10^3 $(x \pm \sigma^a)$
288.15	2.10 ± 0.05	2.41 ± 0.08	1.28 ± 0.01	1.57 ± 0.01
293.15	2.48 ± 0.06	3.04 ± 0.14	1.56 ± 0.01	1.86 ± 0.01
298.15	3.00 ± 0.09	3.84 ± 0.17	1.92 ± 0.01	2.30 ± 0.01
303.15	4.07 ± 0.07	4.58 ± 0.18	2.23 ± 0.02	2.72 ± 0.01
308.15	4.64 ± 0.09	5.94 ± 0.06	2.73 ± 0.01	3.42 ± 0.05
313.15	5.81 ± 0.07	7.27 ± 0.02	3.15 ± 0.07	4.06 ± 0.03
318.15	6.84 ± 0.09	8.84 ± 0.02	3.84 ± 0.03	4.54 ± 0.04

[a] Standard deviation.

Table 2-1: Experimental Mole Fraction Solubility of Water in Studied PFCs

Positron lifetime measurements were reported by Dlubek, Saarinen and Fretwell (1997) in the temperature range of 80 – 300 K for both polyethylene and polytetrafluoroethylene (PTFE or Teflon®). Their study aimed at experimentally estimating the crystalline packing density and the site of local free volumes in the crystalline and amorphous phases. They stated that the appearance of holes, which arise due to irregular molecular packing in the amorphous phase and molecular relaxation among the terminal ends of molecular chains, lowers the density in

amorphous polymers by approximately 10% as compared to the same material in a crystalline state. Their overall findings concluded that the average hole size in PTFE is roughly twice the average hole size seen in polyethylene.

Mechanical properties, crystallinity in particular, of PTFE were investigated by Rae and Dattlebaum (2004) by testing in compression at strain-rates between 10^{-4} and $1s^{-1}$ for a temperature range of -198 to 200 ^{o}C. Their focus was on base-line material characterisation and the compressive response of pedigreed PTFE materials. They found the crystallinity of the sample varied depending on the method of measurement used. Prior to this, a similar study by Lehnert et al (1997) investigated the crystallinity of PTFE by four conventional methods, namely wide-angle X-ray scattering (WAXS), nuclear magnetic resonance density (NMR), differential scanning calorimetry (DSC) and infrared spectroscopy (IR). They aimed at conclusively testing all methods for consistency. They also included in their study a comparison of the conventional methods with a procedure based on Raman spectroscopy. They concluded that all the methods employed provided an estimate rather than an accurate measurement of crystallinity in PTFE.

Water absorption and states of water in semi-crystalline poly (vinyl alcohol) films were studied experimentally by Hodge et al (1996) where they observed a decrease in the crystalline fraction due to the addition of water. Their investigation showed that water molecules initially diffuse through amorphous regions within the polymer attaching themselves to hydroxyl side groups. The inter- and intra- molecular hydrogen bonding were disrupted and resulted in the swelling of the polymer. These initial stages of water absorption where water molecules were directly attached to hydroxyl side groups did not contain sufficient structural order to result in a thermal phase transition and remained in the state of non-freezing water. Further diffusion saw small amounts of water molecules arranging themselves in aggregations that possessed sufficient structural order to undergo a thermal phase transition but was not large enough to be influenced by interactions of macromolecules of the polymer, shifting the phase transitions with respect to that of bulk water. The final stage of water diffusion resulted in water existing as free water within the polymer, located in the free volume of the polymer. By water molecules attaching to the hydroxyl side groups of macromolecules, crystallinity was destroyed as the chains were forced to change from a crystalline planar zig-zag configuration to an amorphous one so as to accommodate the effective size increase of the side groups thus destroying the hydrogen bonding of the system which tightly held the chains in a crystalline array.

Thermodynamic analysis of the mutual solubilities of normal alkanes and water were conducted by Tsonopoulous (1999). Calorimetric methods were used to determine and compare solubility of water in different alkanes. This work showed that water solubility in linear, non-polar alkanes was not dependent on pressure. A monotonic increase of water solubility in alkanes was observed with an increase in temperature.

Solvent clustering in membranes was also investigated by Nguyen et al (1995) to determine its influence on membrane transport properties. Infrared spectroscopy, differential scanning calorimetry, X-ray scattering techniques and visual observations were used to evaluate solvent cluster formations in poly (vinyl alcohol) (PVA), poly (dimethylsiloxne) (PDMS) and poly (vinyl acetate) (PVA_c). When saturated with water, PVA_c membranes contain non-freezable and liquid like water molecules in equal amounts. Infrared measurements on PVA_c indicated that monomeric water molecules initially penetrate the membrane and later aggregate to form clusters. Depending on the water content in the membrane, three different states of water molecules were detected in PVA. These were non-freezable, freezable bound and liquid-like states. Membrane selectivity towards water was found to be affected by the formation of clusters. Water clustering in PDMS was evidenced by a clarity change from a clear to an opaque polymer. PDMS-alcohol systems were also evaluated using experimental techniques to evidence alcohol clusters in polymers. Alcohol clustering in PDMS displayed sorption behaviour within the membrane that deviated from the Flory-type behaviour regularly observed for other solvents. The researchers instead showed that the engaged species induced clustering (ENSIC) model correctly accounted for the sorption behaviour of alcohol in PDMS. In attempting to display how clustering affects permeant sorption and diffusion, they obtained two preliminary results. The first indicating a reduction in the mean diffusion coefficient which led to a smaller flux for higher permeant activities than that of constant diffusivity and the other being an increase in the mean diffusion coefficient with increasing activities. Overall, they concluded that clustering of penetrant molecules is not limited to water and hydrophobic membranes. When clustering does occur, sorption, diffusion and permeant properties are affected, however, much more research is required to elucidate effects on membrane properties.

In a more recent study, Sarassin et al (2015) conducted experiments to determine the diffusion coefficients and gas permeability coefficients of methane, carbon dioxide and hydrogen sulphide in polyethylene. This information was then used to determine the solubility of the aforementioned gases in the amorphous phase of the polymer. They observed no coupling effects and concluded that sorption was dependent only on the fugacity of the gas under consideration and the total pressure. They also observed a decrease in gas solubility at high pressures which they attributed to a hydrostatic effect which was independent of the nature of the gas. From these findings they were able to propose a simple model which provided an accurate description of gas solubility from a low to high gas pressure range.

2.7 Summary

Despite the existing variety of studies which employ the use of molecular simulation and in particular Monte Carlo methods to evaluate and verify different thermodynamic properties and hence deduce an understanding of molecular mechanisms, there is still insufficient literature (both experimental and simulation) regarding the clustering of alcohols in polymers. This study aims at contributing knowledge to the existing polymer database in this regard. It employs the Monte Carlo method to evaluate absorption and clustering of methanol in high density polyethylene and polyvinylchloride to inquire into an understanding of the failure mechanisms of the respective polymers when exposed to such solvents.

CHAPTER 3: HARDWARE AND SOFTWARE

"The first law of thermodynamics says that work is indestructible. We who use computers know better." __ Anonymous

3.1 A Brief History of the "Beowulf" Cluster

During the period of 1980 to 1990, important experiments in research and industry resulted in a growing interest in the potential use of cluster computing. Different strategies for parallel processing were explored and this lead to a milestone development of the Parallel Virtual Machine (PVM) where routines could be run on separate computers that were networked together to allow for data exchange and to coordinate their operations. In 1994, the first Beowulf – class PC cluster was developed using a Linux operating system. This project saw the development of Linux Ethernet driver software and various other low-level cluster management tools thus demonstrating the low cost advantages and smooth performance of Beowulf systems for scientific applications in the real-world (Sterling 2002: MIT Press).

3.2 Processing Mechanism

Many computer processors arranged in a parallel configuration serve as a cluster such that many tasks can be completed simultaneously. A central "master" processor is used as a distribution hub to allocate jobs to the other processors. Communication amongst processors is facilitated by an internal network connecting all processors together. This particular set-up is referred to as a "Beowulf" cluster. A "node" consists of a processor and its peripheral connections.

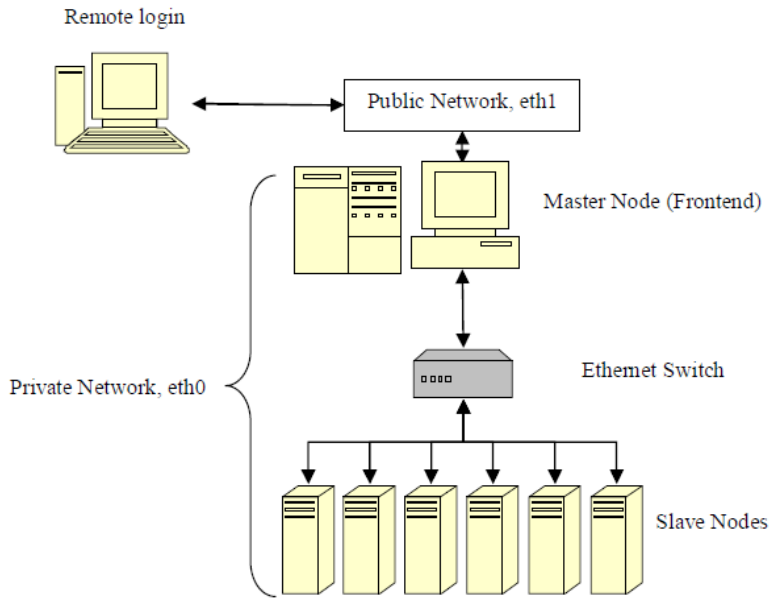

Figure 3-1: Schematic of a beowolf cluster (from Moodley 2008)

The cluster concerned herein is “Lengau” which belongs to the Centre for High Performance Computing (CHPC), an organisation that provides processing support for research groups in South Africa. It consists of a total of 19 racks containing 1008 standard compute nodes (24 cores/node; 24192 total core number; 128 GB memory/node), 5 FAT nodes (56 cores/node; 280 total core number; 1024 GB memory/node) with a total theoretical peak Linpack performance of 774.5 Tflop/s. Interfacing with a cluster was done using a secure-shell login via a “ssh” bash command in the Linux operating system. In instances where a Linux computer was not accessible, “PuTTy”, a hyperterminal program was used which is compatible with both windows XP and Windows 7 operating systems thus direct contact with the cluster itself was not always necessary for the assignment of jobs.

	Lengau Cluster	FAT Nodes
CPU Speed	2.6 GHz	2.2GHz
CPU Model	Intel Xeon (R) E5-2690 V3	Intel Xeon (R) E7-4850
CPU Cores	24192	280
Number of Nodes	1008	5
RAM	126 TB	5 TB
Rpeak	1006 TFlops	
Rmax	782.9 TFlops	
Interconnect	FDR Infiniband Network	FDR Infiniband Network

Table 3-1: Specifications of the beowulf cluster “Lengau”

3.3 Monte Carlo for Complex Chemical Systems (MCCCS) Towhee

Towhee is a Monte Carlo simulation code that was originally designed for the prediction of fluid phase equilibria using the Gibbs ensemble and atomistic force fields. The algorithms particularly focused on addressing molecule conformation sampling. Towhee is designed for compilation in a Unix style environment but can also be compiled on a Windows machine. Towhee is a popular tool for the prediction of thermophysical properties using Monte Carlo molecular simulation. (see URL reference – sourceforge)

As will be discussed in more detail in Chapter 4 (Theory and Methods), the Monte Carlo molecular simulations following the Metropolis Scheme are concerned with the application of random moves to randomly selected molecules, in order to minimise the Gibbs free energy of the system. This was achieved in the present study using the computer programme MCCCS Towhee. The implementation of the Metropolis scheme is shown in the algorithm flowchart following:

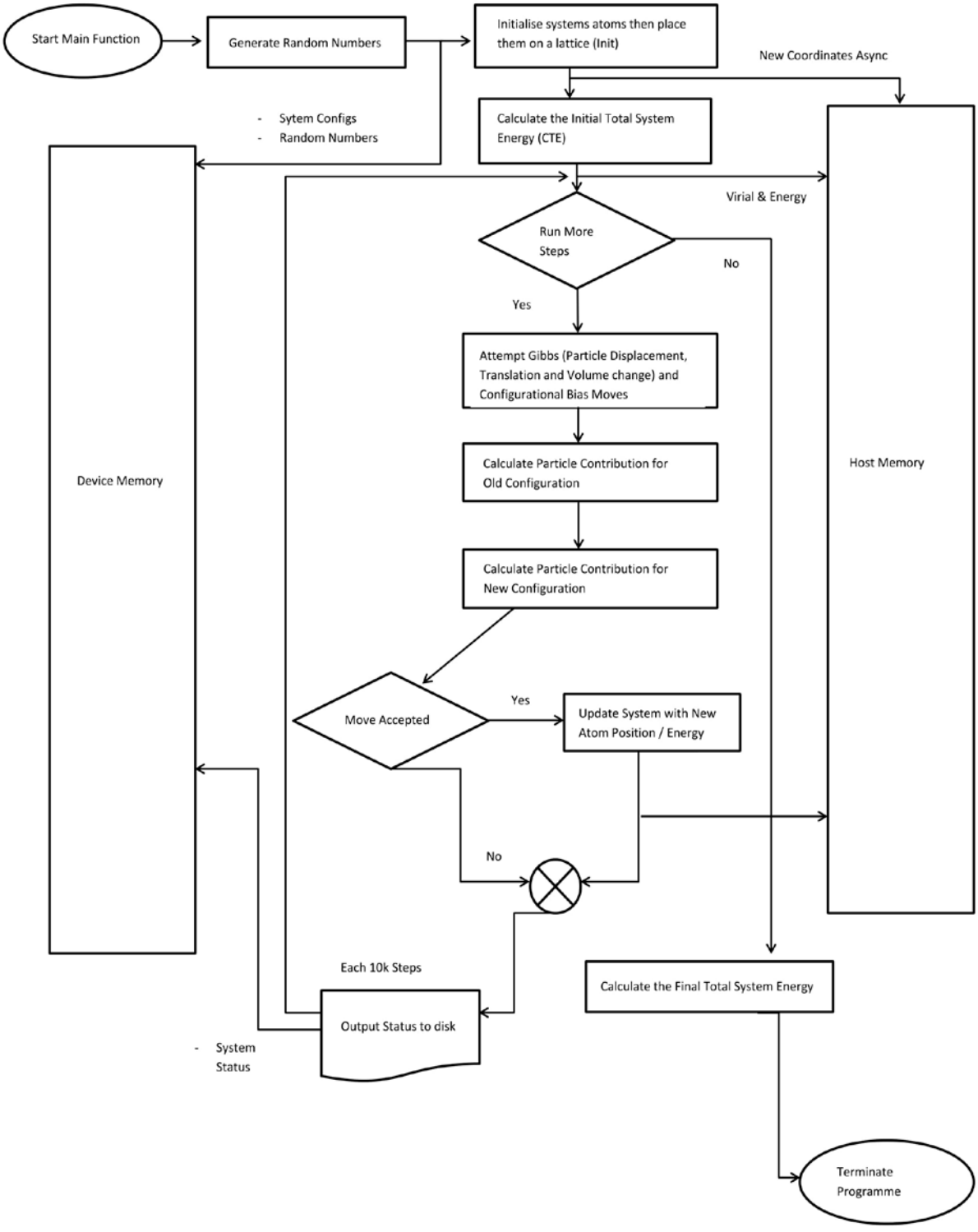

Figure 3-2: Flowchart of the Monte Carlo algorithm as implemented in Towhee

It can be noted that Figure 3-2 shows the procedure to be undertaken for a single calculation run (i.e. the calculations associated with a single attempted change to the configuration of the system.) In practice, this routine is repeated millions of times such that a sufficient number of moves have been accepted so that the system has reached an energy minimum.

3.4 Matlab Coding

An existing Matlab code was modified and used in this study to perform cluster analysis. The analysis considered sampled molecular configurations. For each configuration every methanol molecule in the polymer was compared with every other molecule in the same phase in the same configuration to determine whether the Stillinger criterion was satisfied. A distribution of cluster types could thus be determined for each configuration and collated for all sampled configurations. (see URL reference – Mathsworks)

CHAPTER 4: THEORY & METHODS

"It is a capital mistake to theorise before one has data. Insensibly one begins to twist facts to suit theories instead of theories to suit facts." __ Sherlock Holmes

Statistical mechanics forms the link between macroscopic thermodynamic quantities and the microscopic behaviour of particles. Consider a crystalline solid; to model the behaviour of this material in response to temperature, it can be considered that the most important degree of freedom which allows the atoms to respond to thermal energy changes is the vibration about their rest positions. The vibrational energy of each atom can be quantised since atomic oscillation, in the crystal lattice, is constrained to bonding of the centre around at-rest positions.

4.1 Microstates

In a given system, a collection of microstates is called an ensemble. Considering again an isolated system of three atoms, the diagram below illustrates the possible sets of microstates.

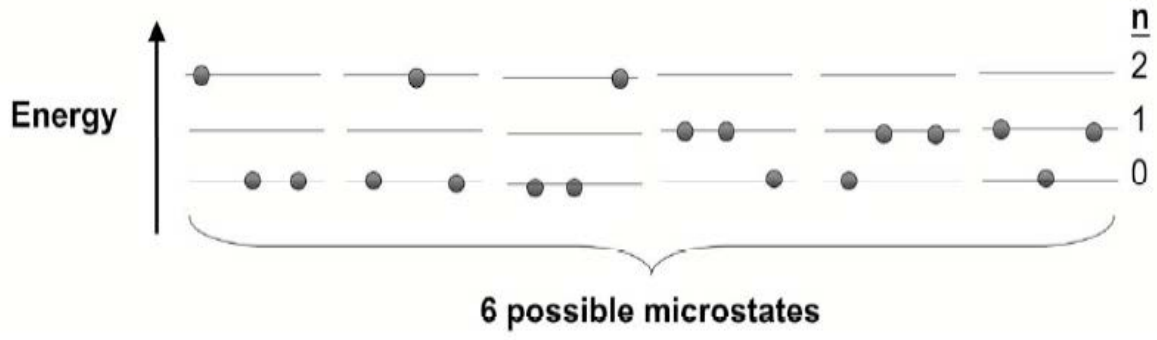

Figure 4-1: Energy level diagram (from Irvine and Marzani 2005: 1-12)

When modelling real systems there exists two cases where atoms may be uniquely identified. The first case refers to distinguishable atoms such as a crystalline solid where each atom is identified by its position in the lattice (x, y, z) and the second case refers to indistinguishable atoms such as gas molecules in a container which only allows the unique microstates to be observed.

Figure 4-2 below shows the individual microstates placed into two groups identified by the number of atoms found in each energy level (n_0, n_1 and n_2). This set of microstates having a given set of occupied numbers is called a State (as opposed to a microstate). The symbol, W, is used to denote the total number of distinguishable states.

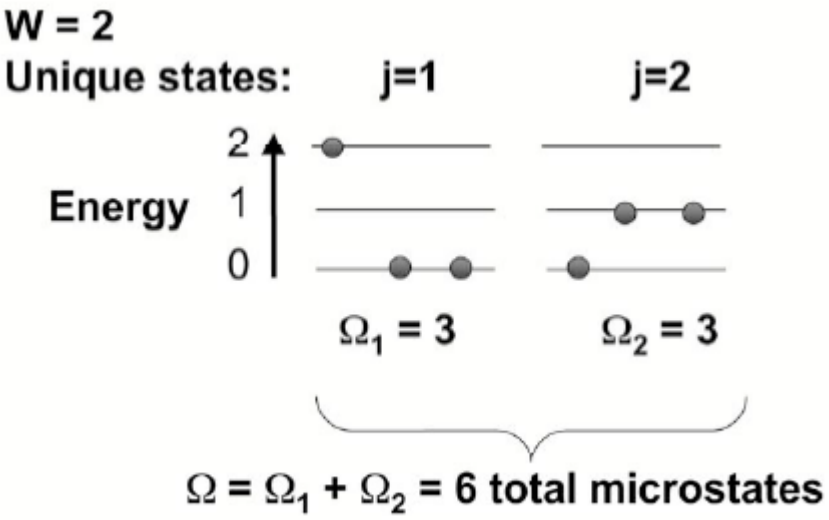

Figure 4-2: Energy level diagram showing unique states (from Irvine and Marzani 2005: 1-12)

The number of distinct arrangements in this very simplified 3-atom model is very small. In a material containing a mole of atoms at room temperature, there exists a large number of ways in which the energy levels can be occupied. Therefore, instead of creating diagrams of the many possible microstates, the focus becomes the probability of finding a particular set of microstates (j) in the ensemble that have a given distribution of the atoms among the energy levels. (Irvine and Marzani (2005: 1-12))

4.2 Basic Postulates of Statistical Mechanics

As stated previously, statistical mechanics forms a link between macroscopic properties and microscopic behaviour. Within this theoretical framework there are two main postulates which are described below;

(I) In an ensemble where Ω (number of microstates) is very large at fixed (U, V, n) each allowed microstate is equally probable.

This postulate explains that microstates having the same energy (U), volume (V) and number of particles (n), occur with the same frequency in an ensemble. Mathematically this is described as:

Probability of each microstate = $p_j = \frac{1}{W}$ (Eq. 1)

Where W = a State

(II) The ensemble average of a thermodynamic property is equivalent to the time-averaged microscopic value of that property for the real system.

This second postulate connects ensemble averages to measured thermodynamic quantities. It explains that thermodynamic properties of a material can be calculated if there exists a model that describes the possible microstates of the system. For example, if measurements were taken on a real system, imagine the atoms of the system undergoing thermal fluctuations that allow the system to rapidly fluctuate between various microstates in the model. This makes the tie average measurement on the real system equivalent to averaging the property in the ensemble of microstates in the model. Assuming the probabilities of each microstate (p_j) have been determined, the average over the microstates of the ensemble can be determined.

Ensemble Average of X = $\langle X \rangle = \sum p_j X_j$ (Eq. 2)

Where: X is the value of X in state j

P_j is the probability of state j

Furthermore, the second postulate states that the average property over the ensemble is equivalent to the measurable thermodynamic quantity in a real system.

Example:

$$\text{Pressure} = \langle P \rangle = \sum pjP_j \qquad \text{(Eq.3)}$$

4.3 Contributions to the Intramolecular Potential Energy

An important factor for the use of molecular dynamics and energy minimisation is to determine the structure for new molecules. The Universal Force Field (UFF) as described by Rappè et al (1992) and used in this study, uses general rules to estimate force field parameters based on the element, its hybridization and its connectivity. The key aspect to predict the energies of an unknown structure is dependent on the accuracy of the force field. A superposition of different two-body, three-body and four-body interactions can be used to describe the potential energy for a molecule of arbitrary geometry. The sum of the valence and non-bonded interactions is used to express the total potential energy as follows:

$$E = E_R + E_\theta + E_\phi + E_\omega + E_{vdw} + E_{el} \qquad \text{(Eq. 4)}$$

The bond stretching is described by the Universal Force Field as either a harmonic oscillator:

$$E_R = \frac{1}{2} k_{ij} (r - r_{ij})^2 \qquad \text{(Eq. 5)}$$

or as the Morse Function:

$$E_R = D_{ij} [e^{-\alpha(r-rij)} - 1]^2 \qquad \text{(Eq. 6)}$$

A bond angle occurs naturally when 3 or more atoms or groups of atoms join. Electrostatic interactions as well as the geometry of surrounding atoms or molecules result in minor

variations to this value. A small cosine Fourier expansion in θ is used to describe the angle bending term as follows:

$E_\theta = \frac{Kijk}{n2}[1- \cos(n\theta)]$…..(linear) (Eq. 7)

and

$E_\theta = k_{ijk} [C_o + C_1\cos\theta + C_2\cos2\theta]$ …..(non-linear) (Eq. 8)

Torsional energy describes the potential energy associated with the twisting of two adjoint pairs of atoms or pseudo-atoms

The small cosine Fourier expansion in ϕ describes the torsional form as:

$E_\phi = K_{IJKL} \sum C_n \cos n\phi_{IJKL}$ (Eq. 9)

A one or two-term cosine Fourier expansion in ω is used to describe the inversion energy of an atom bonded to exactly 3 other atoms as:

$E_\omega = K_{IJKL} (C_o + C_1\cos\omega_{IJKL} + C_2\cos2\omega_{IJKL})$ (Eq. 10)

Non-bonded interactions are described in the Universal Force Field by a Lennard-Jones 6-12 type expression:

$E_{vdw} = D_{ij} \{-2 [\frac{xij}{x}]^6 + [\frac{xij}{x}]^{12}\}$ (Eq. 11)

The valence parameters discussed thus far do not include partial charges. When included, the electrostatic interaction is expressed as:

$E_{el} = 332.0637 (\frac{QiQj}{\varepsilon Rij})$ (Eq. 12)

4.4 Contributions to the Intermolecular Potential Energy

Fundamental physics describes the intermolecular interaction, which is the energy associated with collections of molecules, in terms of van der Waals forces and Pauli repulsion where each describes long range forces and short-range repulsion respectively. The van der Waals attractive forces are as a result of the movement of electrons between the atoms. The van der Waals forces and effectively the Pauli repulsion for a system can be determined from the following correlation:

$$U_{LJ} = 4\varepsilon \left[\left(\frac{\sigma_{ij}}{r_{ij}}\right)^{12} - \left(\frac{\sigma_{ij}}{r_{ij}}\right)^{6}\right] \qquad \text{(Eq. 13)}$$

The above equation was developed by Lennard-Jones (1931). This Lennard-Jones potential describes the interaction between two uncharged molecules or atoms. Figure 4-3 below illustrates that the Lennard-Jones potential is mildly attractive for the approach of uncharged molecules or atoms from a distance but strongly repulsive as the molecules or atoms get very close.

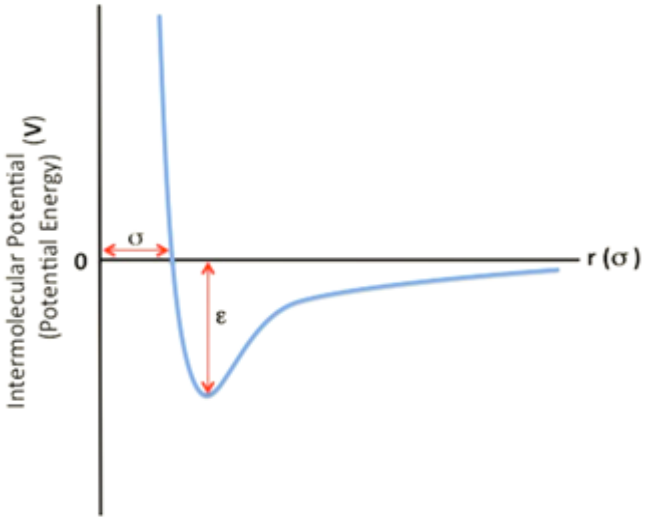

Figure 4-3: Lennard-Jones potential

Note that the deeper the well depth (ε), the stronger the attractive interaction between the two particles. When the bonding potential energy is equal to zero, the distance of separation (r) will be equal to σ.

This attractive force at larger distances can be explained by the *induced dipole-dipole moment interaction* of particles. Dipoles are electrical structures where charges of opposite signs (positive or negative) but with equal magnitudes are separated along an axis. The measure of the strength between the charges is referred to as the *dipole moment* and this strength can be increased by increasing the magnitude of each charge in the dipole or by an increase in separation. The subjection of molecules with dipole moments to an electric field allows the dipole to orient along that field. (see URL reference)

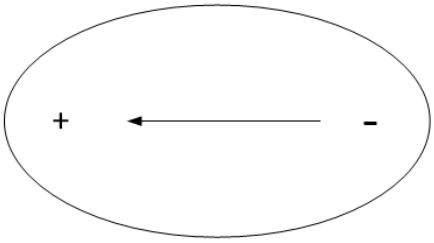

Figure 4-4: A dipole. The arrow defines the direction of the dipole from the negative to the positive charge

For an uncharged atom, there is an electron cloud surrounding the nucleus which is symmetrically distributed thus no dipole moment exists as charges are not concentrated in any particular direction.

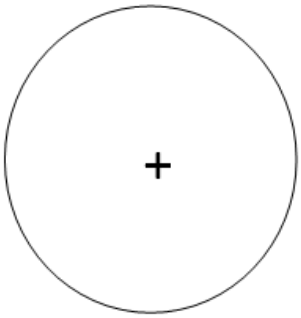

Figure 4-5: An uncharged atom with a positive centre and a negative charge symmetrically distributed around it

Since particles in a liquid are in constant motion, collisions with other particles are also constantly occurring. As two uncharged particles approach each other the symmetry of their electron cloud deforms causing each particle to acquire a dipole moment. This is known as an *induced dipole moment* and lasts for a relatively short period of time as particles approach and dipoles become attracted to each other. This attraction is the van der Waals force.

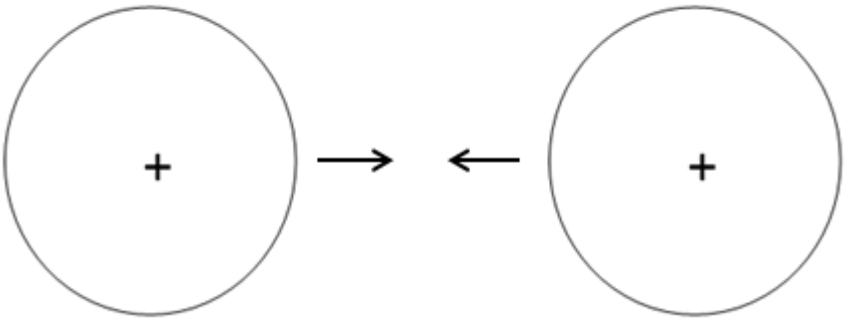

Figure 4-6: Uncharged particles approaching each other

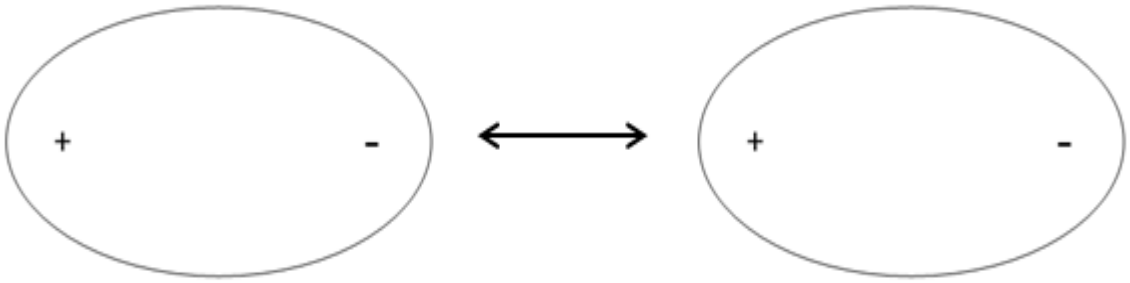

Figure 4-7: Electron clouds deform during collisions resulting in the creation of dipole moments and a weak attraction between particles

4.5 Ensembles

Ensembles are defined as sets of macroscopic variables that are held constant; there are however, many microscopic configurations that correspond to a given macrostate. Recalling the Gibbs Phase Rule, only certain variables can be held constant at once. Other ensembles include the Canonical, Isobaric-Isothermal, and Grand-Canonical ensembles. The Canonical ensemble, also abbreviated as the "NVT" ensemble since the number of molecules in the system (N), the volume of the system (V) and the system's temperature (T) are fixed. Molecular displacement is permitted in terms of molecular translation and orientation. The isobaric-isothermal or "NPT" ensemble fixes the number of molecules (N), temperature (T) and pressure (P) of the system. For this type of system, volume fluctuations are permitted as well as translation and rotation of molecules. This ensemble is more accurate at mimicking the behaviour in physical laboratory experiments. The grand-canonical ensemble or "μVT" ensemble is used to describe the system's behaviour when molecules are inserted into a closed volume where chemical potential must be maintained. For such an ensemble, the volume (V) and temperature (T) and chemical potential are fixed.

4.6 Gibbs Ensemble Monte Carlo

The Gibbs Ensemble Monte Carlo method, developed by Panagiotopoulos (1987) specifically characterizes phase transitions. This method divides each phase into a "box" where three types of perturbations can be performed. Gubbins' (1993) descriptions of these moves are given below:

4.6.1 Particle Displacement

Molecules are randomly displaced such that thermal equilibrium is achieved within each region. This is achieved by the movement of a particle to a new, random location within the original "box". The Metropolis Monte Carlo algorithm is applied to obtain the particle moves and the system is essentially at constant NVT. The acceptance or rejection of the displaced particle is dependent on the probability determined by the following equation:

$$\mathcal{P}_{move} = \frac{\exp(-\beta Enew)}{\exp(-\beta Eold)} = \exp(-\beta\Delta E) \qquad \text{(Eq. 14)}$$

Where ΔE describes the change in configurational energy determined from each move.

Figure 4-8 below illustrates this move.

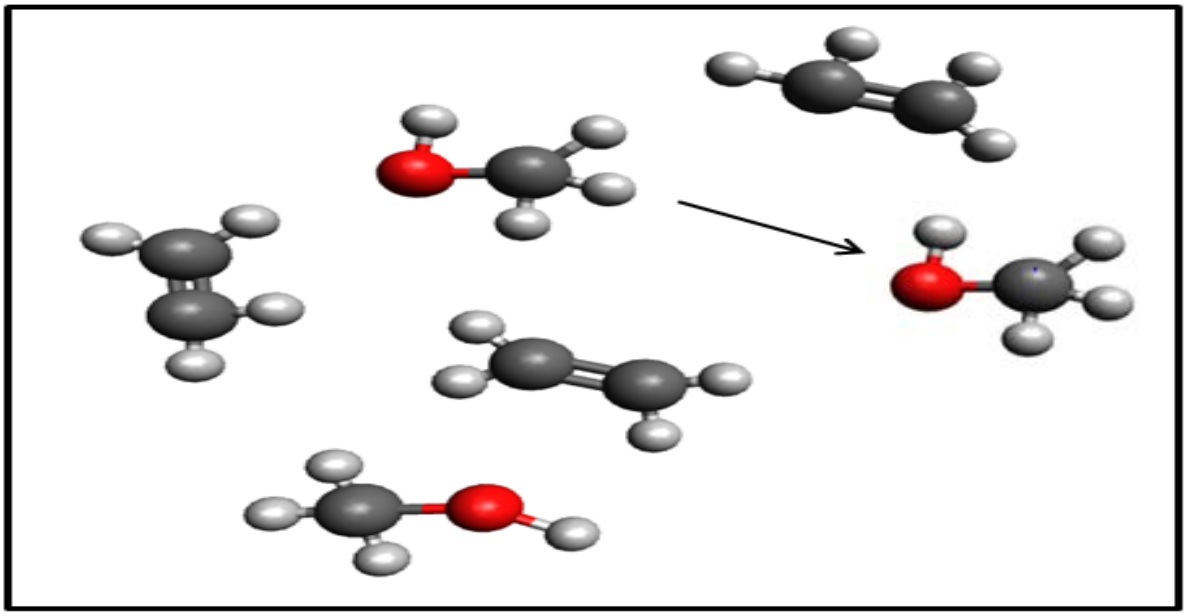

Figure 4-8: Illustration of Monte Carlo particle displacement within each phase

4.6.2 Volume Change

Pressure is maintained by the equal and opposite change in volume in each region. There exists two methods in which the Gibbs Ensemble Monte Carlo algorithm is applied with regards to changes in volume. One method is to couple the volume changes such that the total volume of the system is kept constant (NVT). Using this approach, the volume of both "boxes" is simultaneously adjusted so as to conserve the total system volume thus an increase in the volume of "box 1" is combined with a decrease in volume of the same amount in "box 2". The probability to accept or reject the volume perturbation is obtained via the following equation:

$$\mathcal{P}_{Volume} = \exp\left(-\beta\left[\Delta E^1 + \Delta E^2 - N^1 k_B T \ln\frac{V1+\Delta V}{V1} - N^2 k_B T \ln\frac{V2+\Delta V}{V2}\right]\right) \quad \text{(Eq. 15)}$$

Where 1 and 2 refer to "box1" and "box2" and k_B is the Boltzmann Constant.

The second approach does not couple the changes in volume but maintains both "boxes" at the same pressure (NPT). The volume of each "box" is varied independently to ensure the criterion of constant pressure is met. The probability of the acceptance or rejection of the change is determined by the following equation:

$$\mathcal{P}_{Volume} = \exp\left(-\beta\left[\Delta E^1 + \Delta E^2 - N^1 k_B T \ln\frac{V1+\Delta V}{V1} - N^2 k_B T \ln\frac{V2+\Delta V}{V2} + P(\Delta V^1 + \Delta V^2)\right]\right) \quad \text{(Eq. 16)}$$

Where 1 and 2 refer to "box1" and "box2" and k_B is the Boltzmann Constant.

Convergence can be obtained at a faster rate by varying the volume of one "box" at a time rather than each box simultaneously. In this instance, the probability equation is simplified to:

$$\mathcal{P}_{Volume} = \exp\left(-\beta\left[\Delta E^1 - N^1 k_B T \ln\frac{V1+\Delta V}{V1} + P\Delta V^1\right]\right) \quad \text{(Eq. 17)}$$

Where 1 refers to the "box" undergoing a volume change and ΔE is the change in configurational energy.

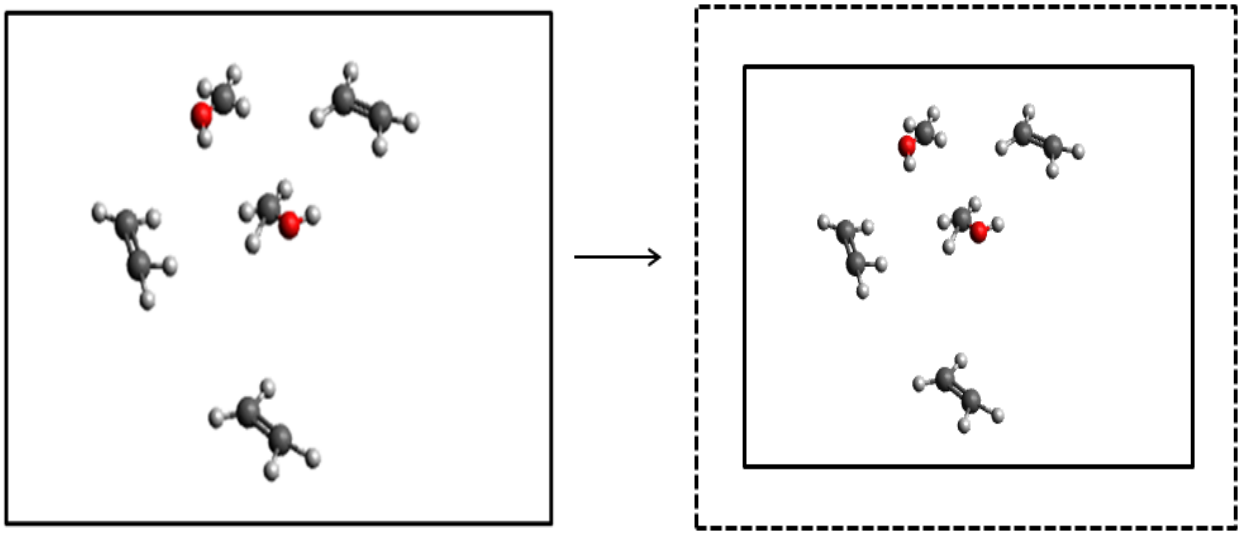

Figure 4-9: Illustration of before and after Monte Carlo volume change for one "box" in the NPT Gibbs ensemble

4.6.3 Particle Transfer

This is the equalisation of chemical potentials of each component in either region via the random transfer of molecules. The transfer is accomplished by the creation of a particle in phase one (i.e. "box1") and the simultaneous destruction of a particle in phase two (i.e. "box2"). The two "boxes" are at the same temperature and in both "boxes" the chemical potential of each component is equalised via the transfer move. The coexisting phases are thus representative of the Grand Canonical Ensemble. The probability to accept or reject the transfer perturbation is obtained via the following equation:

$$P^{1}_{Tansfer} = \exp[- \beta\Delta E^{1} + \ln(\frac{zV1}{N1+1})] \quad \text{(Eq. 18)}$$

$$P^{2}_{Tansfer} = \exp[- \beta\Delta E^{2} + \ln(\frac{zV2}{N2+1})] \quad \text{(Eq. 19)}$$

$$P_{Transfer} = P^{1}_{Tansfer} \times P^{2}_{Tansfer} = \exp\left(-\beta[\Delta E^{1} + \Delta E^{2} + k_B T \ln\frac{V2\,(N1+1)}{V1N2}\right]), \quad \text{(Eq. 20)}$$

where the activity coefficient z is expressed by:

$$z = \exp(\beta\mu)/\lambda^{3} \quad \text{(Eq. 21)}$$

λ is the de Broglie wavelength of constituent particles and μ is the chemical potential.

At high densities, the implementation of the Gibbs ensemble method is problematic as the interchange of molecules becomes very difficult. Such a disadvantage is shared with other methods such as the Grand Canonical Monte Carlo method and the NPT and Test Particle method.

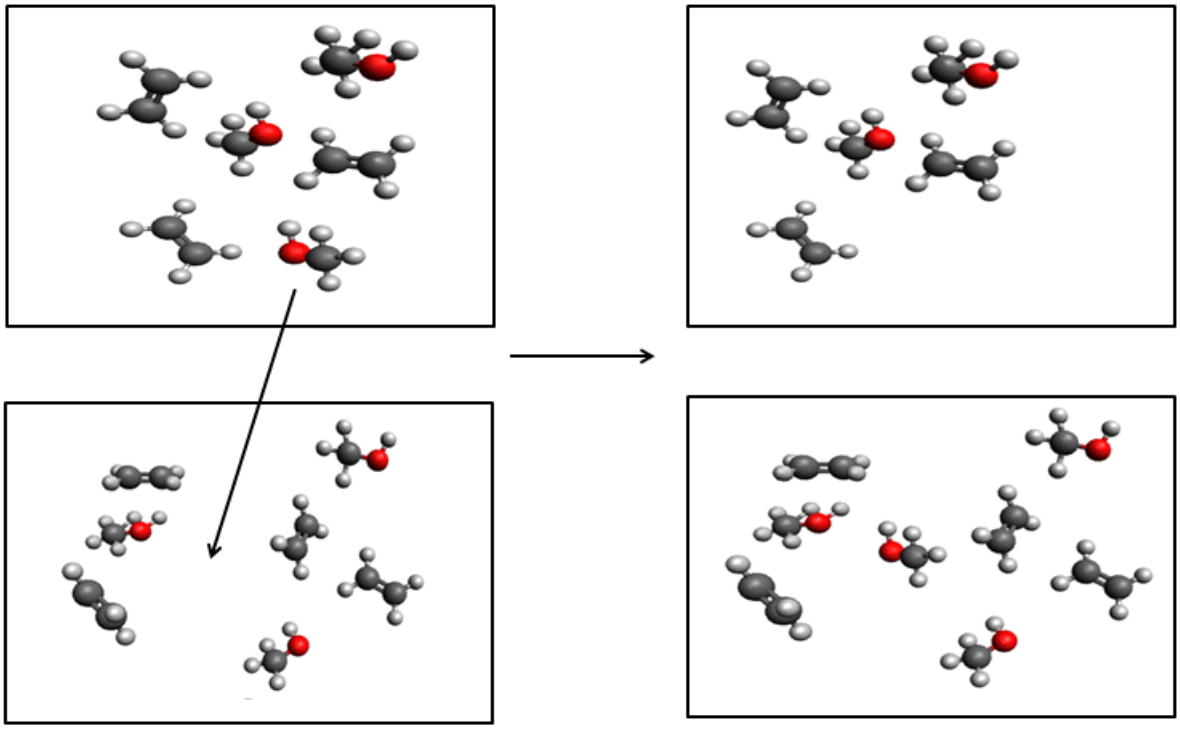

Figure 4-10: Illustration of Monte Carlo particle transfer between phases

A problem related to the simulation of systems consisting of hundreds or thousands of molecules is that a high proportion of the molecules would lie at the outer most surface of the system if it were a free standing system. This would over emphasise surface effects at the expense of bulk properties. To visualise this problem consider a drop of water and a cup of water; in the drop of water the surface area to volume ratio is much higher than in a cup of water. The Gibbs Ensemble overcomes this by situating multiple simulation boxes in the bulk material thus emulating it by application of boundary conditions.

4.7 Configurational-Bias Monte Carlo (CBMC)

A common issue faced during simulations of large, complex molecules is the high likelihood of rejection of large molecules being inserted or displaced. This is a result of the displacement of one molecule being very dependent on the acceptance of the displacement of all its constituent atoms. The works of Rosenbluth and Rosenbluth (1955) and Siepmann (1990) resulted in the configurational-bias method to overcome such issues. The approach is such that a section of a molecule is deleted and then "regrown" elsewhere. The regrowth can be biased by, for example, restricting torsional angles to reasonable bounds, in order for energetically reasonable conformations to be produced using the method. The following main steps describe the configurational-bias Monte Carlo algorithm. Initially, part of a molecule is deleted. This is followed by a regrown 'trial' conformation using a Rosenbluth scheme and a Rosenbluth weight of the new configuration. The Rosenbluth weight for the old configuration is calculated by 'retracing' the original conformation. The Rosenbluth weights of the old and new configuration are compared to determine if the energy of the system has decreased to an acceptable amount. The CBMC technique facilitates the transfer between phases through regrowth since transferring a large molecule between phases with its configuration intact would have a very low acceptance rate.

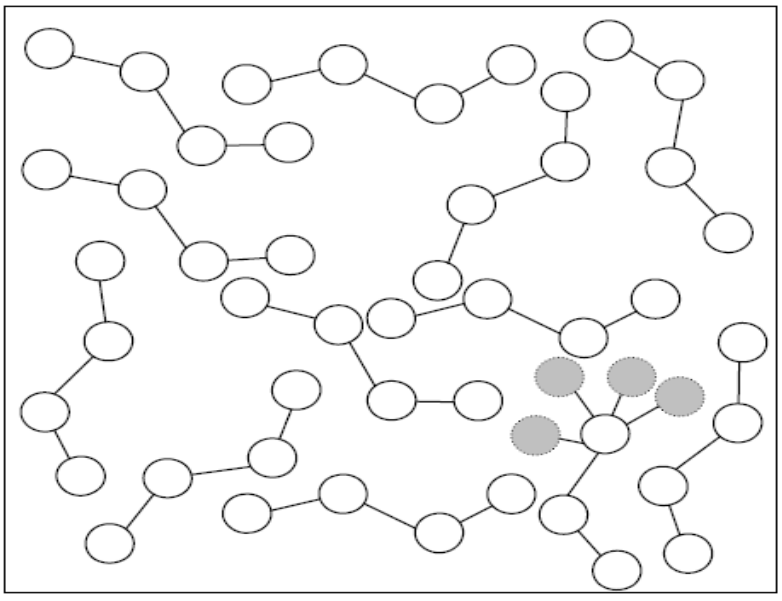

Figure 4-11: Configurational Bias Monte Carlo method. The regrowth of the molecule is completed by placing the next atomic group at the most energy-favourable position in space (from Moodley 2008)

4.8 General Moves

In addition to the standard Gibbs Ensemble moves to which the molecules were subjected, various other moves were also applied to the molecules in order to achieve equilibrium. These moves are described and illustrated below.

Pivot: One interaction site is rotated around the axis it shares with an adjacent interaction site to find the lowest energy.

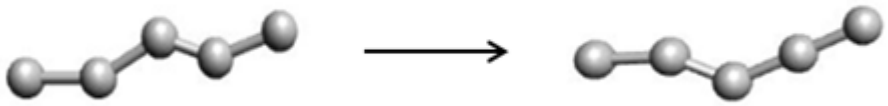

Figure 4-12: Illustration of the pivot move

Intramolecular Translation: An interaction site within the molecule is translated linearly while retaining its connections with adjacent sites to find the lowest energy.

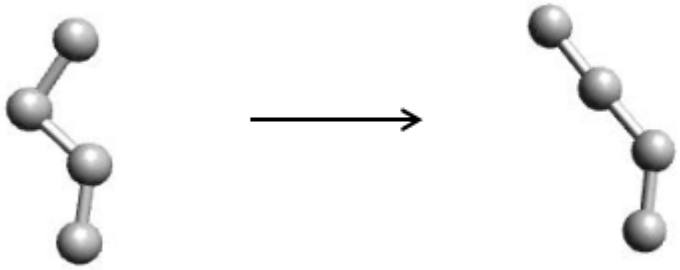

Figure 4-13: Illustration of the intramolecular translation move

Rotation: The entire molecule is rotated around its centre of mass using several trial configurations to find the lowest energy.

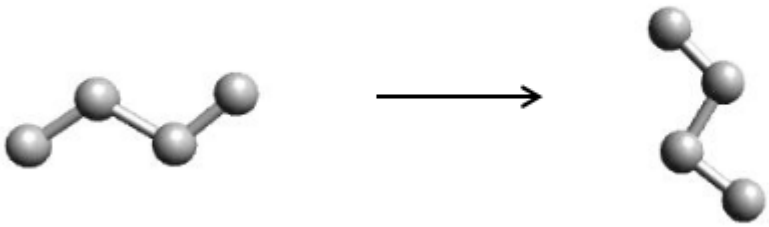

Figure 4-14: Illustration of the rotation move

Centre of Mass Translation: The entire molecule is translated linearly using the centre of mass as a reference point, while maintaining its orientation, to find the lowest energy.

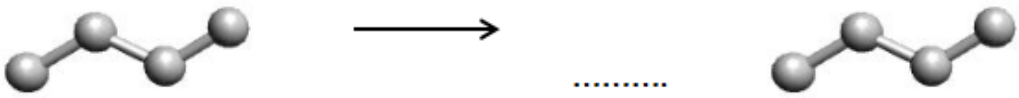

Figure 4-15: Illustration of the centre of mass translation move

Although the above moves are inherent in the Gibbs ensemble perturbations, they are also considered general moves since they can be applied to other ensembles.

4.9 Configurational Bias (CB) Moves

In addition to the Gibbs Ensemble moves to which the molecules were subjected, various configurational bias moves were also applied to the molecules in order to achieve equilibrium. These moves are described and illustrated on the next page.

Configurational Bias Regrowth: This involves the regrowth of molecules using several trail configurations to determine the lowest energy.

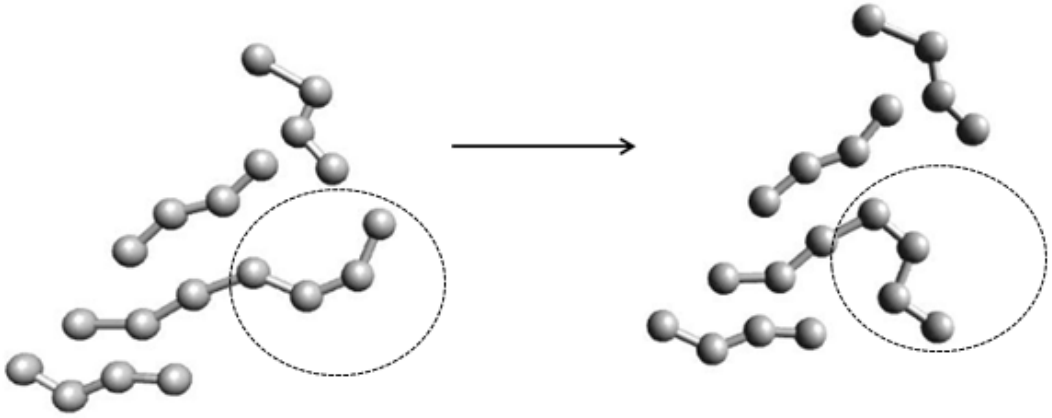

Figure 4-16: Illustration of the configurational-bias regrowth CB move

Configurational Bias Regrowth (Box Swap): This involves the regrowth of molecules, in the second box, using several trial configurations to determine the lowest energy.

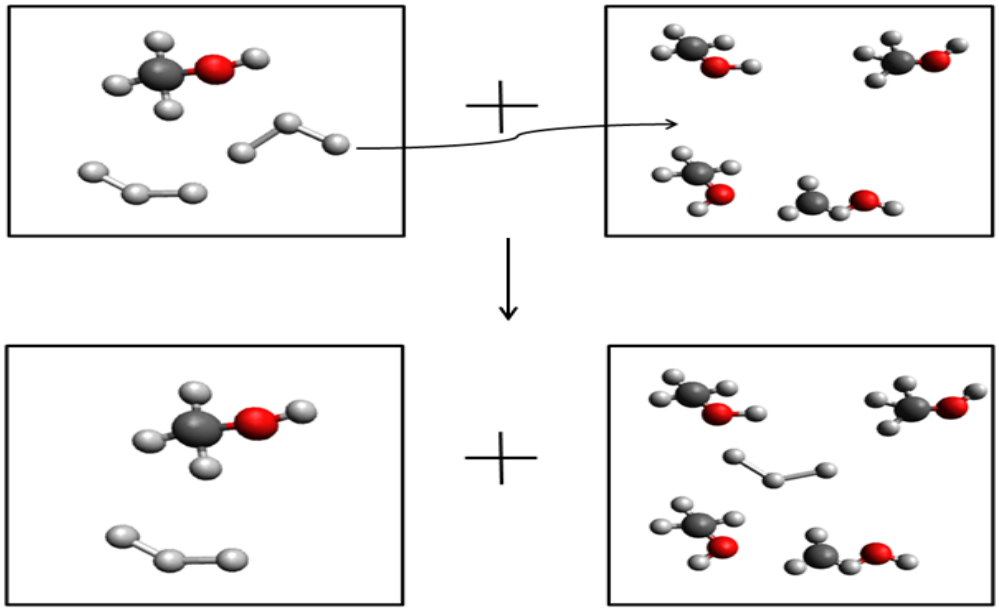

Figure 4-17: Illustration of the configurational-bias regrowth (Box Swap) CB move

4.10 Cut-Off Radius and Boundary Conditions

It can be seen that an increase in intermolecular distance (well beyond the collision radius σ) results in a decrease in the magnitude of the Lennard-Jones potential such that at an energy contribution of a few σ there is a negligible effect upon individual molecules. A cut-off radius is thus implemented (which also reduces computational demands), where beyond this, intermolecular interactions are no longer explicitly calculated. Mathematically, this can be described as for $r > r_c$ (where r_c equals the cut-off radius) the intermolecular potential is set to zero. This was necessary as in order to calculate the total interaction on a molecule by every other molecule two separate summations were required where each summation considers the van der Waals and electrostatic contributions respectively. The cut-off radius denotes the region, within the box under consideration, where the total van der Waals contributions are considered. Periodicity errors can be avoided by setting the cut-off radius to less than half the length of one side of a cubic box. An analytical correction term may be added to the total energy at the end of a simulation, to account for molecular interactions beyond the cut-off radius. Frenkel and Smit (2001) stated that this correction term assumes number density to be the same on either side of the cut-off radius. This correction term applies only to the van der Waals forces as they interact in a short range. For long-range interactions, the correction term is determined by the Ewald summation technique and is considered by Frenkel and Smit (2001) to be highly accurate. This move is only used when molecules have partial charges. The algorithm, however, consumes a major portion of the processing time. This is a trade off in return for high accuracy. In this study a cut-off radius of 14 Å was employed.

Periodic boundary conditions are applied to allow for the simulation of systems containing limited number of molecules, in modelling bulk fluids. A periodic boundary condition is created by replicating a simulation box (the box that contains molecules to be simulated) in all dimensions surrounding the box.

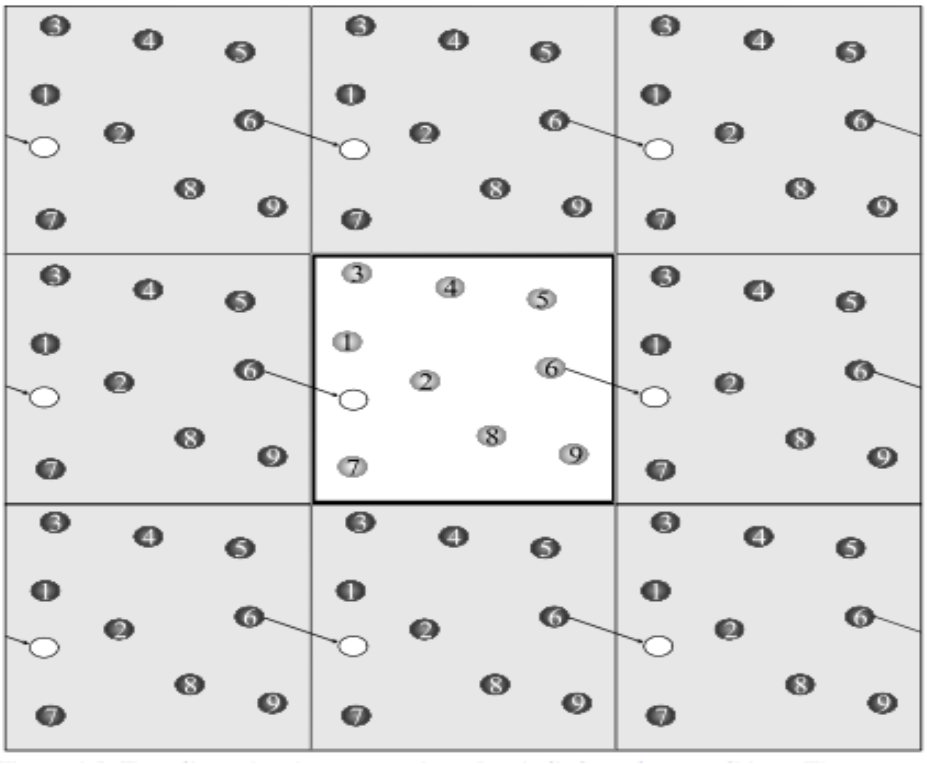

Figure 4-18: Two-dimensional representation of periodic boundary conditions where the centre cell is the simulation cell and the surrounding cells contain the periodic images of the molecules within the simulation cell. (fromWoller (1997))

By doing this, an interacting molecule is unable to interact with molecules outside a box of the same size as the simulation box but still centred at the interacting site. This prevents molecules located near the box boundary from experiencing conditions very different from those found at the centre of the box. The aim of the method is to prevent a molecule from interacting with one or more of its periodic images which, according to Allen and Tildesley (1987), introduces an artificial periodicity in the system causing it to become an ordered system rather than a random system which would render incorrect statistical results. A consequence of the periodic boundary condition is that transferring molecules across a boundary causes the molecules image to revert into a simulation cell on the opposite side.

4.11 Cluster Definition

The definition of the cluster may significantly influence the results obtained from any cluster analysis. Definitions from literature may consider intermolecular distances or intermolecular energy or both. The cluster definition to be used in this work is that proposed by Stillinger (1953), which is one of the earliest definitions and which uses a distance-based criterion of an intermolecular distance of approximately 1.5 times the Lennard-Jones size term (i.e. 1.5σ) of the molecule under consideration. This definition proposed by Stillinger is a simple and intuitive tool in the identification of clusters: two atoms are considered to be clustered together when their centres of mass are a distance of less than a predefined radius apart from each other. In addition, each molecule can only belong to one cluster. This predefined distance is referred to as the Stillinger radius (r_s). (see Wedekind and Reguera (2007) for additional discussion on this issue).

Since an all-atom force field was used, the application the Stillinger (1953) definition was not straightforward. Therefore a pseudo-Lennard-Jones size parameter was fitted to the intermolecular potential computed for the all-atom methanol molecule. This was achieved by using Avogadro, a cross-platform, open source advanced molecule editor and visualizer (see URL references). Two methanol molecules were constructed with the centres of mass fixed in place, and the constituent atoms were rearranged until the lowest energy of the configuration was achieved. In this way, the lowest energy configuration for specified values of the intermolecular separation was achieved. The distance between the centres of mass of each molecule was determined using a built-in function. This procedure was then repeated to produce a table of energy (kJ/mol) and distance (Å) values. Using this data and the Lennard-Jones equation, a graph of potential energy versus distance was produced from which the Lennard-Jones parameters (σ, ε) were obtained through least-squares fitting. Figure 4-19 illustrates the result.

Methanol molecules in their all atom representation present a situation where there are many degrees of freedom to re-arrange two molecules even in a dimer configuration. The three possibilities include methyl-alcohol, methyl-methanol and alcohol-alcohol. Consequently the approach taken in this study may favour one particular dimer configuration however to determine this would require a detailed ab-initio study which is beyond the scope of this study.

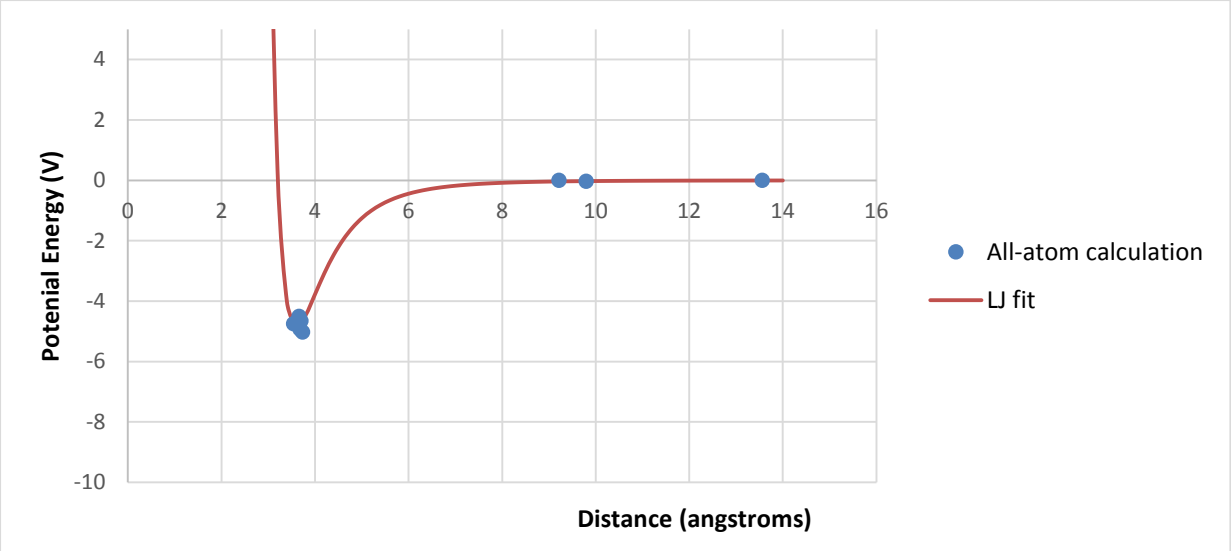

Figure 4-19: Lennard-Jones parameters

4.12 Experimental Method

Absorption measurements at atmospheric pressure were also conducted as a means of comparison to the simulations that were subsequently performed. Both high density polyethylene and polyvinylchloride sheets were cut into strips to obtain a volume of approximately 0.0075cm^3 per strip. The strips were weighed using an Adventurer® scale manufactured by OHAUS, prior to being placed in an alcohol solution. The strips were placed in glass vials and filled with methanol to ensure that the entire strip of polymer was submerged in the alcohol. The vials were placed in different water-baths at temperatures of 25^{o}C, 30^{o}C and 40^{o}C, respectively, for 24 hours at atmospheric pressure. Thereafter the strips were removed, dabbed dry with tissue paper and weighed again. The amount of methanol absorbed could then be estimated as an average of three experimental runs per polymer, per temperature value. High Density Polyethylene was manufactured by AKS Lining Systems (Pty) Ltd and Polyvinylchloride was manufactured by Maizey Plastics. Both polymers were of commercial grade. The methanol used in the experimental tests was produced by Sigma-Aldrich and was 99.8% pure.

CHAPTER 5: RESULTS AND DISCUSSION

"Accept your genius and say what you think." __ Ralph Waldo Emerson

5.1 Simulation Protocols

Although Towhee can readily generate initial configurations via configurational-bias, an attempt at faster initialisations for the simulations was attempted in this study. This entailed generating templates of the polymer molecules using Avogadro, in order for Towhee to create an appropriate simple cubic lattice for the initial configuration. A template is a single polymer molecule in an energy optimised structure which Towhee would duplicate at the lattice points to initiate a simulation. While only marginally reducing simulation times,this approach yielded an unacceptably low regrowth move acceptance rate (less than 0.01%). To correct this, a different approach was attempted. In the second approach, configurational bias was used to generate the molecules in a lattice that was slightly bigger than the original lattice from the template and this resulted in much higher acceptance rates for regrowth moves and a much higher rate of convergence. Regrowth acceptance rates in HDPE varied up to 40% for a 3-atom segment of polymer chain to about 0.1% for the entire molecule which is a much better regrowth rate than the rate of 0.01% achieved when using the template. In PVC the regrowth rate was about 0.3% for the entire molecule. Regrowth moves are very efficient when accepted because they generate a representative view of the system that is more naturalistic (i.e. the random shapes of molecules). These observations may be pertinent to other researchers undertaking simulations of polymeric systems using Monte Carlo simulations.

5.2 Trial Simulations and Force Field Validation

Pure species simulation systems consisting of PVC and HDPE were conducted at 298.15 K and 1 atm initially. These systems contained polymers with chain lengths of 50 carbon atoms and 20 carbon atoms for both polymers. The density from each of these simulations was examined to determine which was closest to the experimentally determined polymer density.

This is because absorption was the phenomenon being considered, which is strongly related to the mass density of the simulated polymer. The density result of the simulations for the 50 carbon atoms showed large deviations from literature density values of PVC and HDPE and had to therefore be discarded. The deviation in density for HDPE and PVC of 50 carbon atoms was 63% and 79% respectively. Much smaller density deviations of 11% and 40%, for HDPE and PVC of 20 carbon atoms respectively, were obtained thus the 20 carbon atoms rendered density values fairly close to those found in literature for each polymer under consideration (the convergence for the 20 carbon atom molecules can be seen in Appendix C). This indicates that polymer chains of 20 carbon atoms represented a more realistic description of the pure polymer systems and were deemed acceptable.

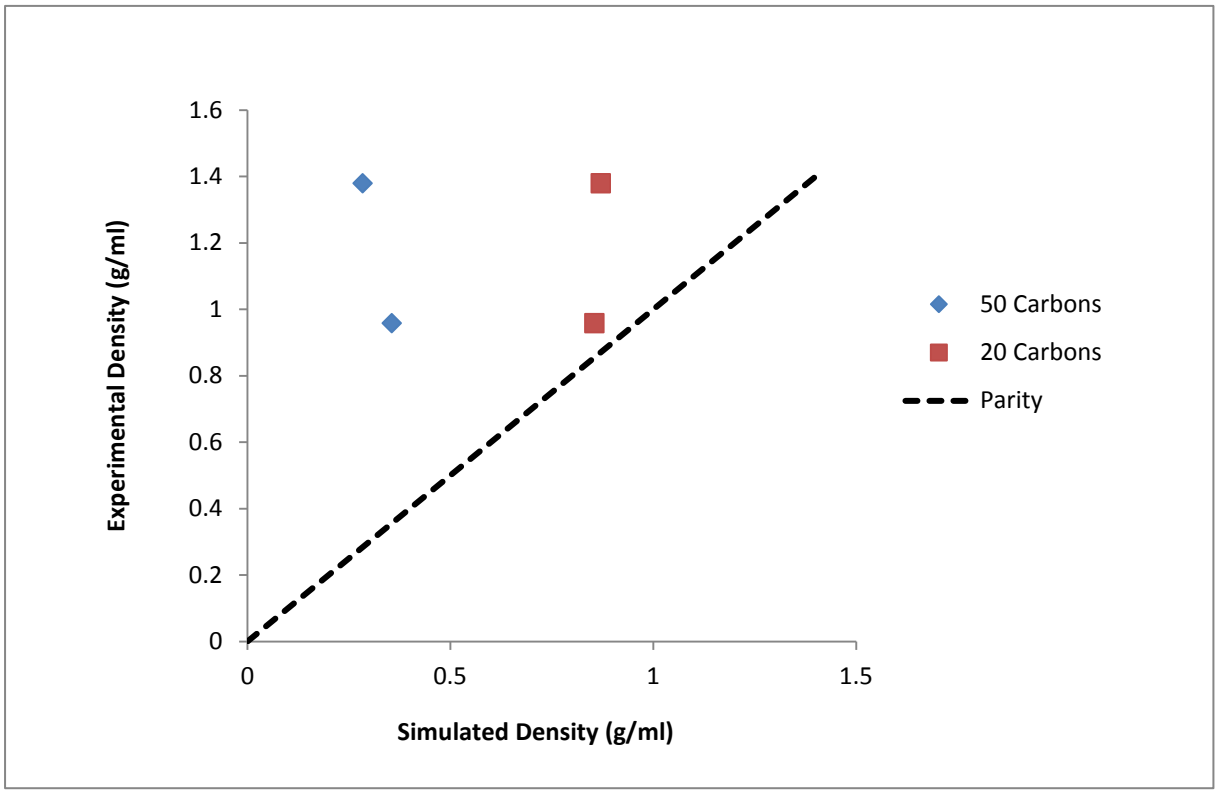

Figure 5-1: Comparison between simulated and experimental density for HDPE and PVC (Note: The upper points represent PVC and the lower points represent HDPE)

In Figure 5-1 above, the parity line is where experimental data equals the simulated results and ideally all data points should lie on this line. It can be seen that the 20 carbon polymers are closer to the parity line than their 50 carbon counterparts. In addition to the issue of mass

density, the distances at which intermolecular interactions occur should be taken into consideration. Generally, the van der Waals forces start becoming negligible in the region of 9 – 14 Å, therefore it is important to have polymer molecules longer than this length to avoid penetrant molecules being able to interact with the entire length of the polymer molecule. Figure 5-2 illustrates this by showing the Lennard-Jones potential for nitrogen, argon and methane; for intermolecular separations greater than about 9 Å, it is apparent that the Lennard-Jones potential rapidly tends to zero. The Lennard-Jones parameters for these gases were obtained from Talu and Myers (2001).

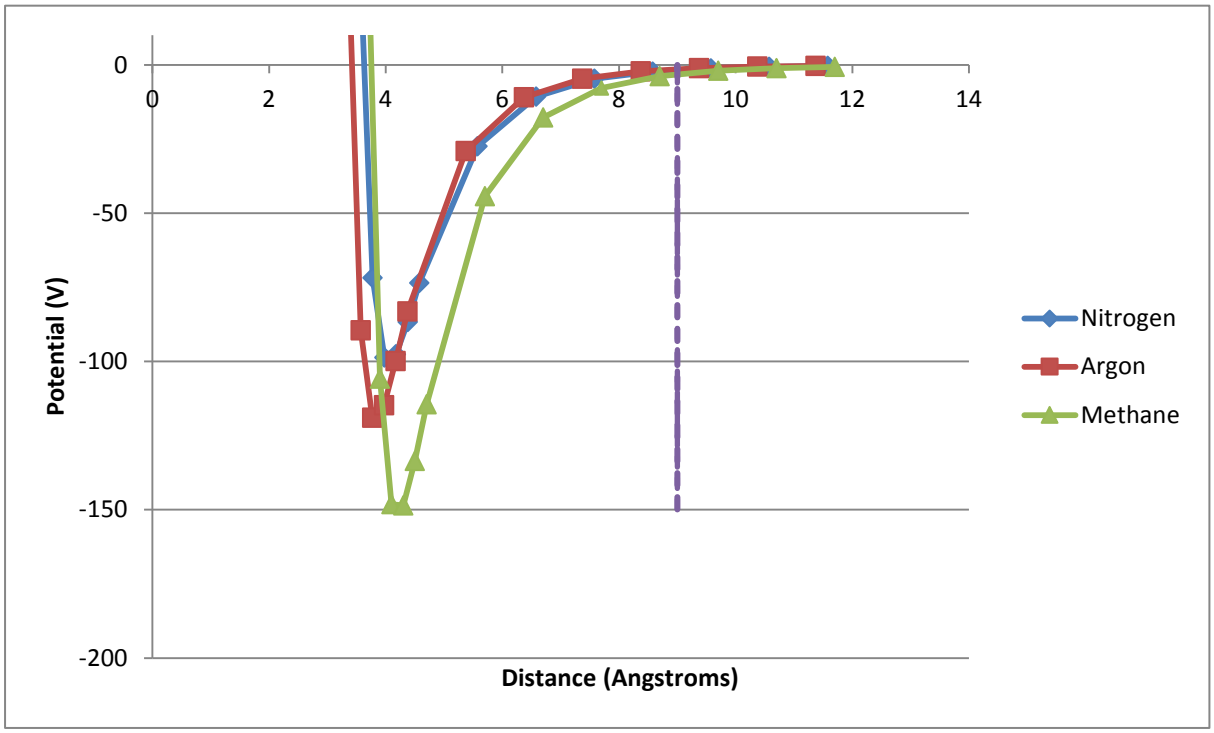

Figure 5-2: Lennard-Jones Potential for nitrogen, argon and methane (The dotted line indicates the tendency to zero at 9 Å)

Since the 20 carbon atoms chain showed a better fit to experimental density data than the 50 carbon atom chain, in terms of mass density it was preferable. The above stated criterion in conjunction with density considerations is important as ideally the simulated system is required to have the correct density whilst also having penetrant molecules only interacting with a portion of the simulated polymer, in order to approximate real intermolecular behaviour.

Generally it may be expected that increasing the chain length may increase the density of the simulated system; however the work of Rahmati et al (2012) has shown this may not necessarily be the case all the time. It was found that the relationship between density and polymer chain length is not monotonic and therefore simply increasing the chain length of simulated polymer chains may not necessarily guarantee a fit to experimental polymer density as shown in Figure 5-3 below. The results from the simulations show a higher density for a chain length of 20 carbon atoms versus a chain length of 50 carbon atoms, which concurs qualitatively with the results of Rahmati et al (2012).

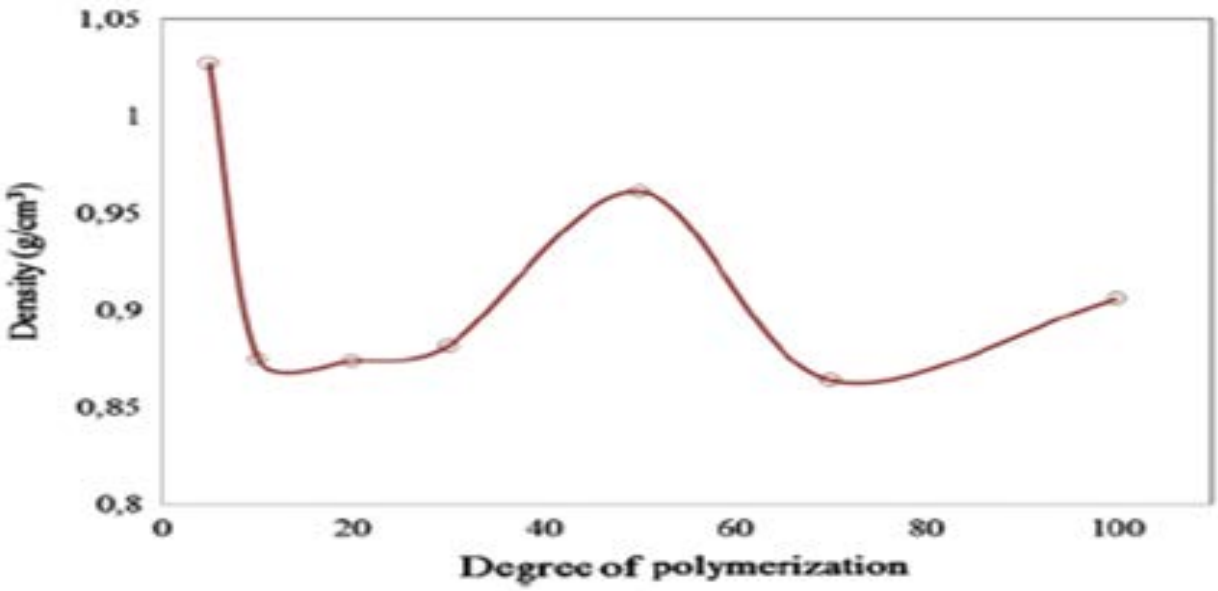

Figure 5-3: Density profile of polyurethane membrane as a function of degrees of polymerization (from Rahmati et al (2012))

5.3 Experimental Results

Figure 5-4 below shows the trends of the results from the experimental testing of absorption of methanol in PVC and HDPE.

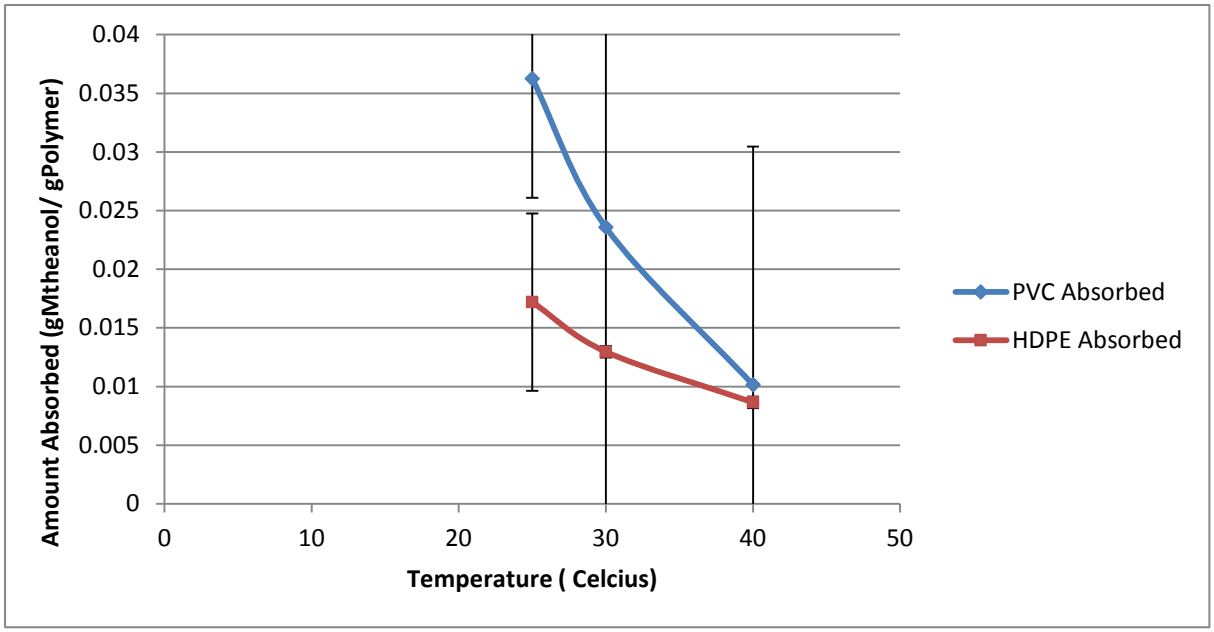

Figure 5-4: Graph of the comparison of the amount absorbed between HDPE and PVC (Experimental)

A decrease in absorption with an increase in temperature is observed. This trend suggests that adsorption rather than absorption is occurring (Atkins 1990). It can be noted that this decreasing trend is observed for both PVC and HDPE, indicating that in both cases, the methanol behaves more like a confined fluid that has been adsorbed as opposed to a fluid absorbed into a liquid-like solution.

5.4 Simulation Results

Figure 5-5 and Figure 5-6 shows results obtained from the simulation runs for HDPE and PVC. The observed trend is a decrease in absorption of methanol with an increase in temperature. For HDPE the decrease in methanol uptake, when going from 25 ^{o}C to 40 ^{o}C, was 4.3% which was higher than the less than 1% change observed for PVC in the same temperature range. This decreasing trend was also observed in the experimental tests.

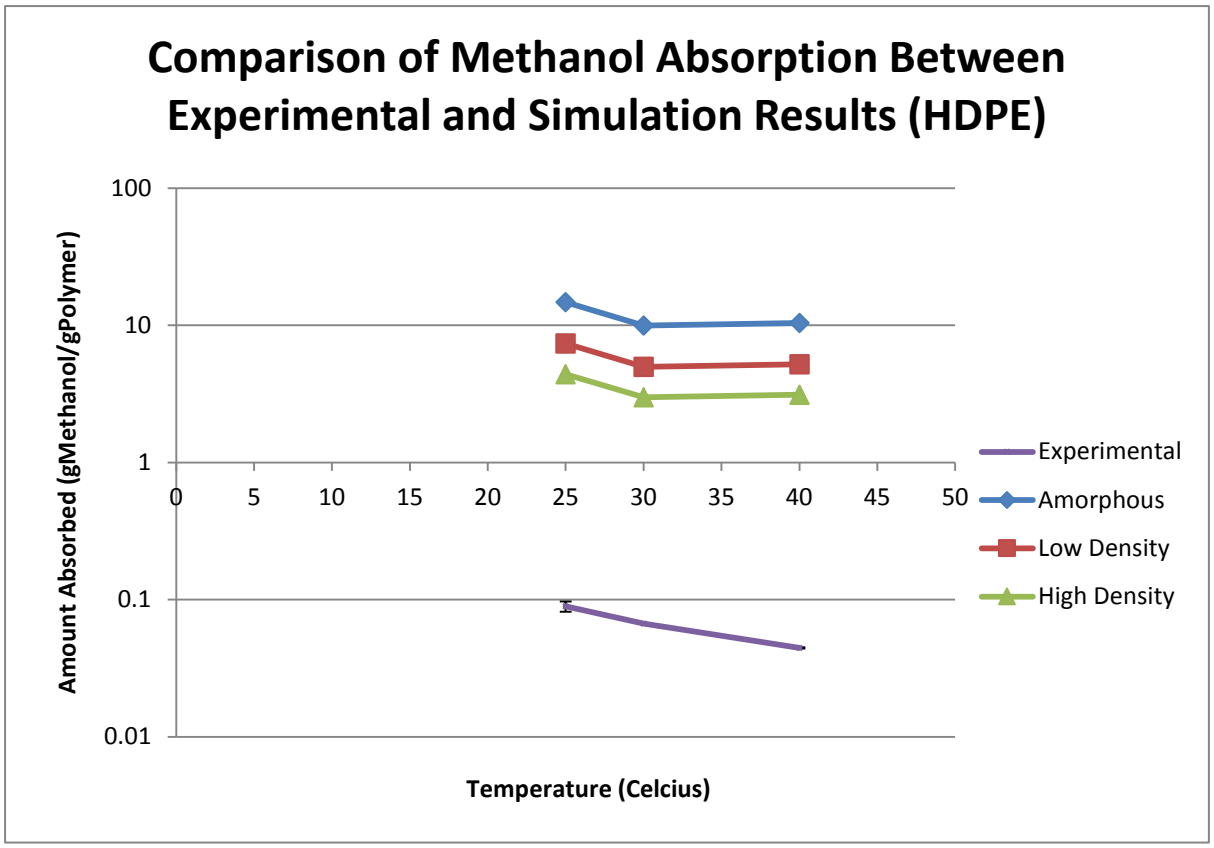

Figure 5-5: Comparison of methanol absorption between experimental and simulation results for HDPE

It should be noted that the error bars for the experimental runs shown in Figures 5-5 and 5-6 are extremely small. The error bars for the amorphous, low density and high density simulations are indistinguishable on the figures as they are much more negligible than that of the experimental runs.

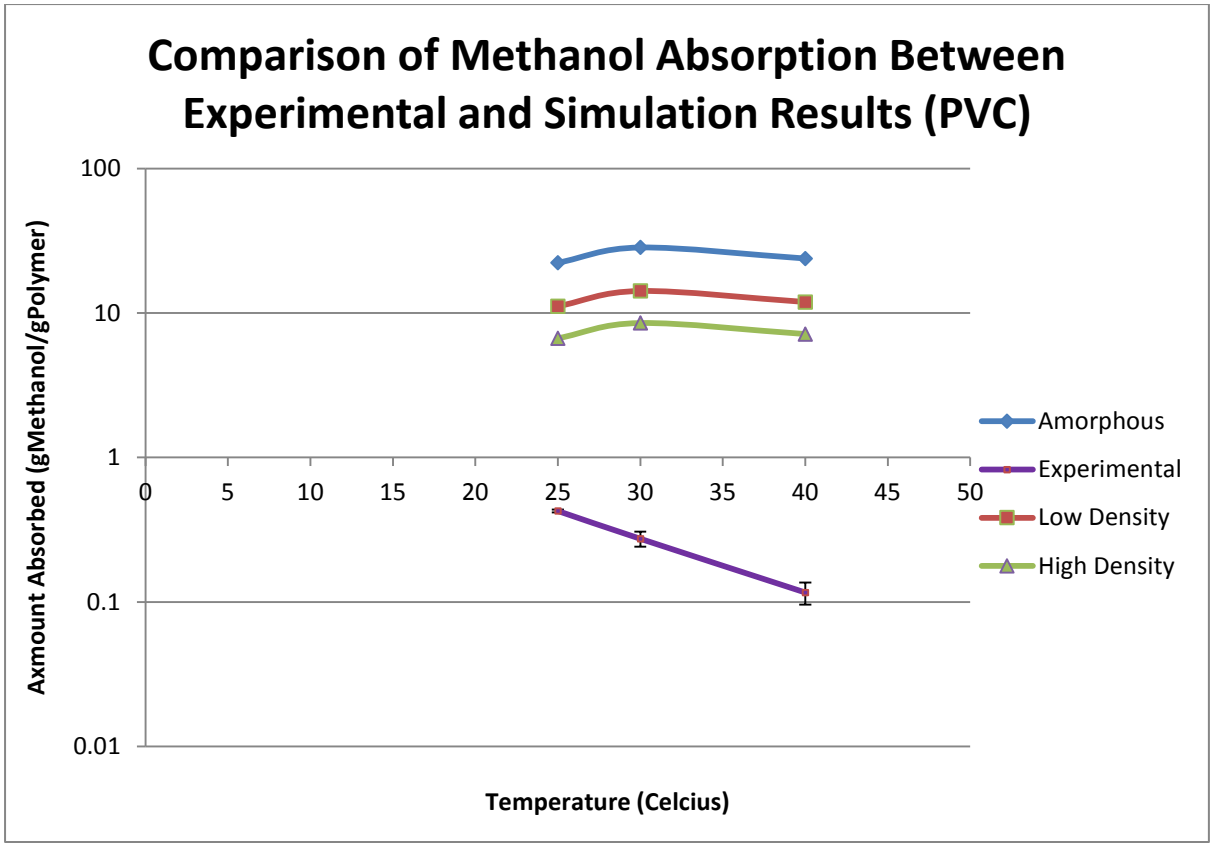

Figure 5-6: Comparison of methanol absorption between experimental and simulation results for PVC

It can be seen that the simulation results show a greater uptake of methanol than that of the experimental results. This suggests that the simulations overestimate the methanol uptake compared to the physical experiments. At 25 ^{o}C, simulations showed a methanol uptake of 14.71 g/polymer for HDPE and at the same temperature laboratory results indicated an uptake of 0.089 g/polymer. This indicates that the simulations are allowing for methanol absorption of more than 100% greater than experimental measurements. Closer inspection showed that this may be attributed to the methanol phase described by the United Force Field which resulted in an overestimate of the fluid density. According to a previous study (Moodley 2008), it is not necessarily possible to describe multiple phases well quantitatively using simple atomistic force fields. Either one phase must be described with very high accuracy, or both (or more) phases will only be matching experimental data moderately well. In the present study, the simulations were employed as a purely predictive tool, and so force field parameters were not fitted to experimental data. In light of the results of the aforementioned

study by Moodley (2008), it may also not be possible to fit parameters to describe both the methanol phase and the polymer phase equally well simultaneously.

The simulation results are adjusted for high and low density because the simulations do not explicitly consider crystalline portions of the polymer but such portions are existent in real polymers. Crystalline regions are too large to be included in simulations relating to a molecular scale. The work of Börjesson et al (2013) also took into consideration the crystalline portion of the polymer when conducting their studies by applying a correction factor to adjust their simulation results. This is shown by Equation 22 which demonstrates the conversion of solubility (S) to account for crystalline portions in a polymer matrix.

$$S = \frac{S^*}{X_{am}} \qquad \text{(Eq. 22)}$$

Where: S^* is the experimentally determined solubility, and

X_{am} is the fraction of amorphous region in the sample

Including crystalline portions explicitly in the simulations would be computationally expensive as these portions are impervious to light penetrant molecules as shown in the work of Pal et al (2005). If a highly crystalline polymer was being simulated, 90 % of the polymer phase may be impervious to the absorption of methanol, which would result in most of the computational time being used to perform calculations for polymer molecules having little to no impact on the uptake of methanol molecules.

The trend evident in both Figures 5-5 and 5-6 indicates that there is a very minor decrease in methanol absorption thus inferring that temperature has little apparent effect on the simulation results for both systems. With regards to the amount absorbed, it was previously stated that the simulations overestimate methanol absorption in both systems but is approximately consistent with the experimental data in terms of the amount of methanol absorbed in HDPE relative to PVC.

The work of Johansson (2007) showed that water clustering in the polymer phase was highly correlated to the density of the water in the polymer phase. This conclusion enables one to predict which polymer may have more clustering when comparing different types of

polymers. In this study, it was expected that dimers would display a higher presence in clusters as the availability of more thermal energy will prevent molecules from “sticking” together. The resultant dispersion would prevent larger cluster formation as they require a higher density.

5.5 Cluster Topologies

In order to recognise and analyse clustering in the polymer matrix, a criterion must be stipulated to determine what constitutes clustering. This was outlined in Chapter 4 in the description of cluster definitions. To recap, it may be stated that methanol molecules that were within 1.5 times the Lennard-Jones size term for the species were considered to belong to a cluster. Additionally, it can be noted that a single cluster may consist of several methanol molecules, arranged in different geometries. The topologies (size, shape, orientation) of the various cluster types analysed in this work are shown in Figure 5-7. The different cluster types may be grouped based on shared topological features as follows:

Linear Clusters: Are those in which the methanol molecules are arranged in straight chains, with no molecules lying perpendicular to the “line” of molecules. In this study, linear clusters are depicted by types 1, 2, and 4 in terms of cluster topologies.

Cyclic Clusters: Are those in which three or more methanol molecules are joined together forming a circular / ring-like structure. In this study, cyclic clusters are depicted by types 3, 5 and 7 in terms of cluster topologies.

Branched Clusters: Are those structures of methanol molecules which have a molecule extending from a linear “string” of molecules. In this study, branched clusters are depicted by type 6 in terms of cluster topologies.

It should be noted that topology type 6 can be considered either branched or cyclic. To further differentiate this type of cluster molecule from others, the presence of a ring as a superordinate criterion was used to explicitly determine cluster topology groupings that are cyclic in nature. Type 6 topology is thus considered a branched cluster type in this study.

In addition to assigning clusters to specific topologies, within those topologies the type of clustering can be further classified into dimers, trimers and tetramers. Type 1 topology is a dimer as they are formed by two molecules joined together. Type 2 and type 3 topologies are trimers since their structure contains only three molecules and the remaining types 4 to 7 are

tetramers as an arrangement of 4 molecules constitute the molecular structure. In a study by Johansson, Bolton and Ahlström (2005), it was seen that increasing the temperature caused clusters to change from having a closed topology or ring-like structure to having a more open topology such as linear or branched chains. Using this result, it may be expected that, in this study, temperature increases would favour the prevalence of a linear dimer topology to other topologies (especially cyclic structures) present in the polymer matrix.

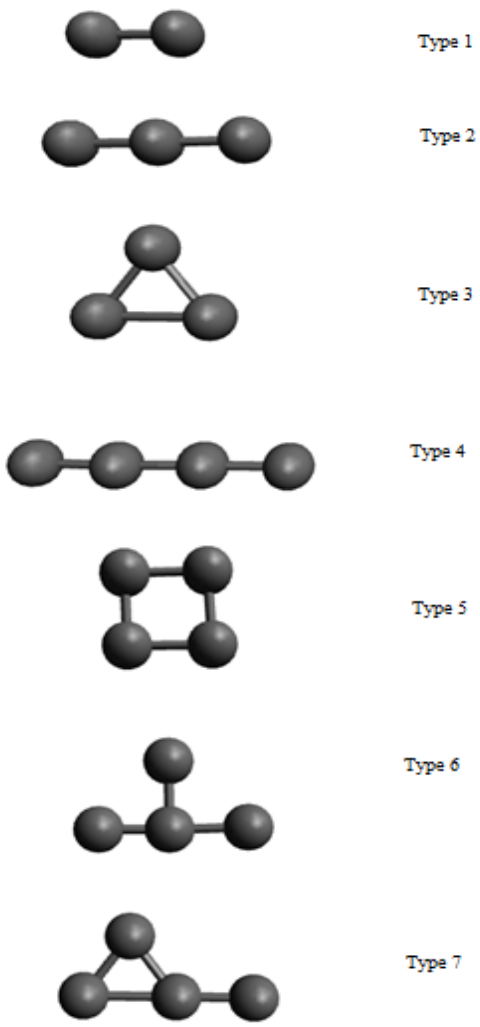

Figure 5-7: Topologies of the various cluster types

5.6 Cluster Analysis

The cluster analysis of HDPE as shown in Figure 5-8 below, illustrates that an increase in temperature results in a decrease in the overall frequency of methanol clustering. The

distribution of methanol molecules in each cluster type can be seen. In addition, overall clustering is also shown as overall clustering is the sum of the number of each type of cluster topology.

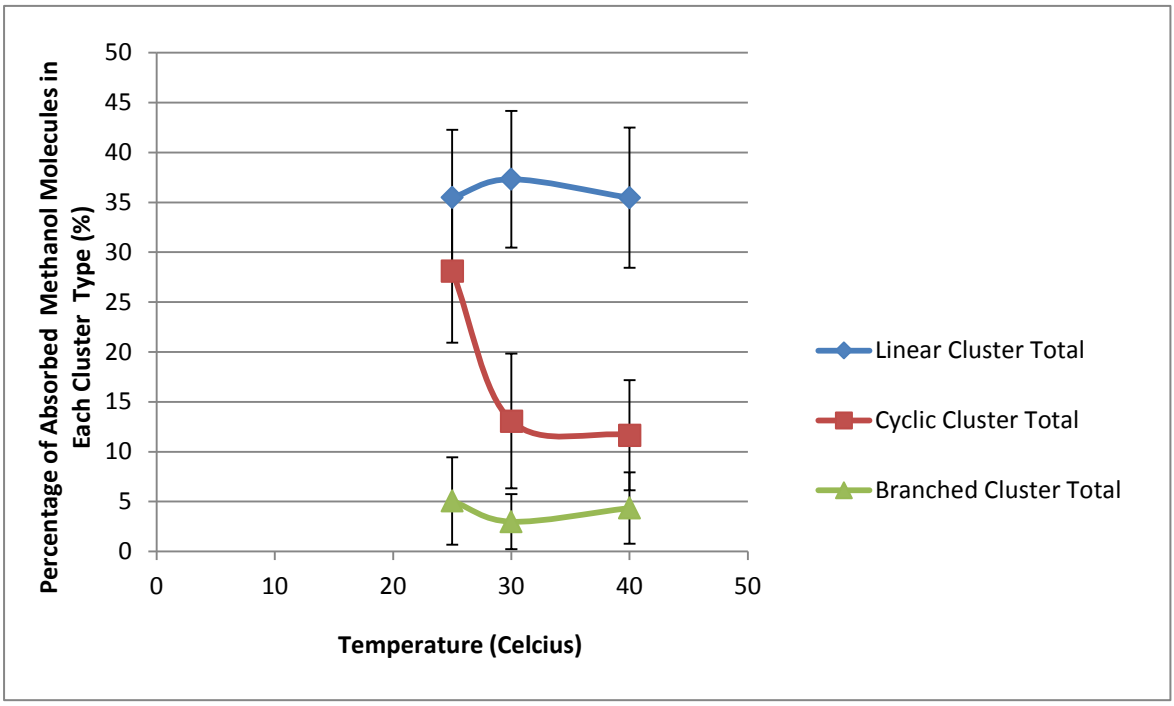

Figure 5-8: Clustering of methanol in different topologies in HDPE as a function of temperature

The uptake of methanol into the polymer matrix of HDPE entailed the formation of more linear clusters than cyclic or branched clusters. Increasing the temperature had a greater effect on reducing the amount of cyclic clusters formed where the percentage of clustering dropped from 28% to 12%. Temperature increase had an almost negligible effect on the linear cluster formation as there was only a 0.01% change overall. The predominant linear clusters found in HDPE are of the type 1 topology. Type 2 and type 4 clusters are also present in the linear clustering but decrease with temperature as opposed to type 1 which displayed an increase with increasing temperature. For the cyclic clustering, type 1, 3 and 7 topologies were all present in the clusters but decreased significantly with an increase in temperature with type 3 being the dominant type in the cluster and type 7 decreasing to zero. The branched clusters showed little variation with very slight decreases and increases in each case.

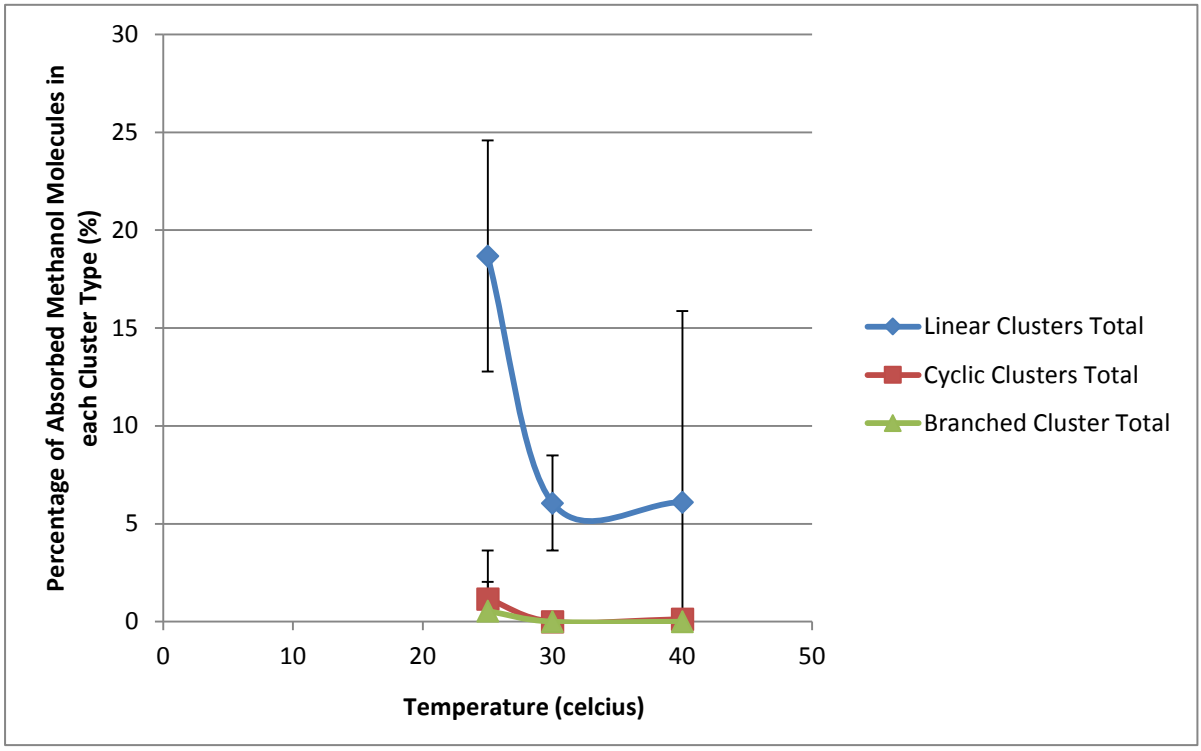

Figure 5-9: Clustering of methanol in different topologies in PVC as a function of temperature

The same trend of decreasing cluster formation as seen with HDPE was also observed for PVC. However, the amount of reduction in clustering was far greater in PVC than HDPE. The formation of cyclic and branched clusters in PVC was reduced to almost negligible amounts of 0.13% to 0% respectively when the temperature of the system was increased from 25 to 40 ^{o}C. This suggests that the chlorine atoms greatly interfere with the clustering process. Figure 5-9 above shows that there was a higher methanol uptake into the PVC polymer matrix than in HDPE which indicates that although methanol may not cause great clustering in PVC, it does result in the polymer swelling up more which also poses a problem for the durability of the material. Type 1 cluster topology was again the predominant topology in the linear clusters and type 2 decreased greatly while type 4 reached zero at 30 ^{o}C. As with HDPE, the type 3 topology was the predominant type in the cyclic clusters with type 7 becoming negligible at 30 ^{o}C. Topology type 5 was not present at all in the cyclic clusters. Negligible amounts of branched clusters were present in PVC.

When comparing the overall clustering of HDPE and PVC, there is initially significantly greater clustering in HDPE than PVC as shown in Figure 5-10 although the percentage of

clusters decreases with an increase in temperature. The percentage of clustering in HDPE decreases from 69% to 51% and in PVC from 20% to 6% as the temperature is increased from 25 ^{o}C to 40 ^{o}C. Since PVC displays much less absorption than HDPE, there is a possibility that the amount of methanol absorbed on a mass basis may increase the propensity of methanol molecules to aggregate into clusters.

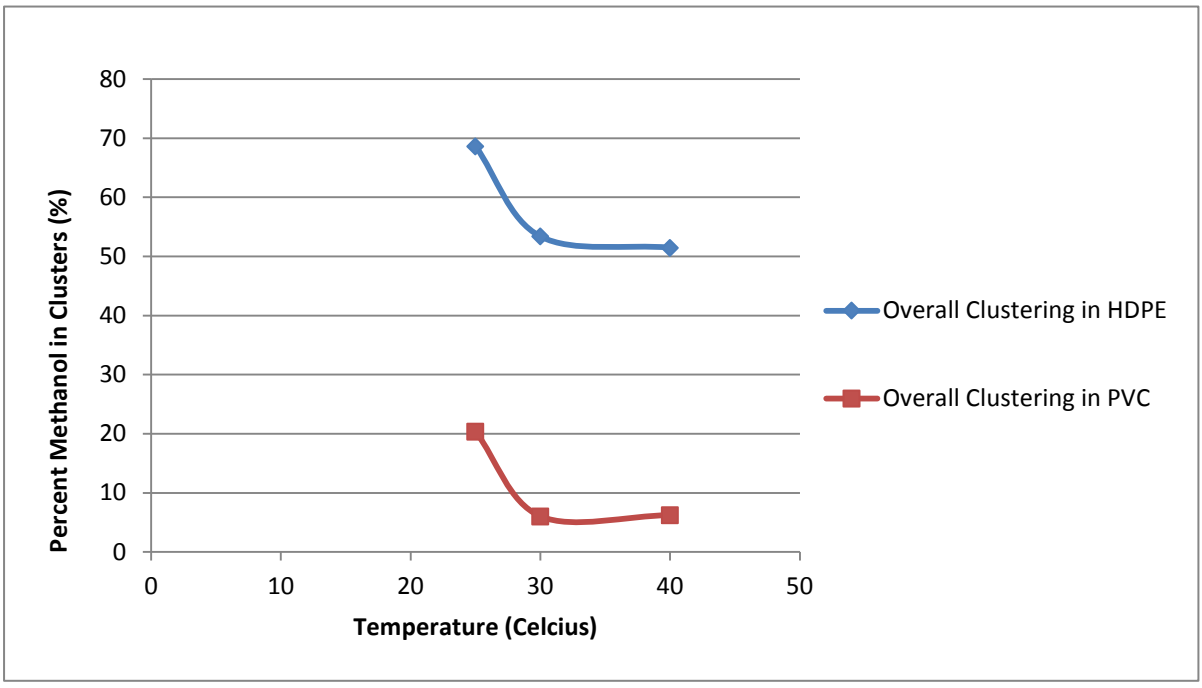

Figure 5-10: Comparison of overall clustering between HDPE and PVC

5.6 Number Density

Number density refers to the number of methanol molecules per unit volume of the polymer phase. The higher the number density, the more closely packed are the methanol molecules in a unit cubed region of the polymer which may indicate a higher likelihood of the occurrence of clustering in that space. This can be a more useful tool than the total amount absorbed when predicting the likelihood of an absorbed species to aggregate into clusters, since molecules such as methanol necessarily need to be in close proximity to form clusters in the first place.

Figure 5-11 shows the number density versus overall clustering in HDPE and PVC.

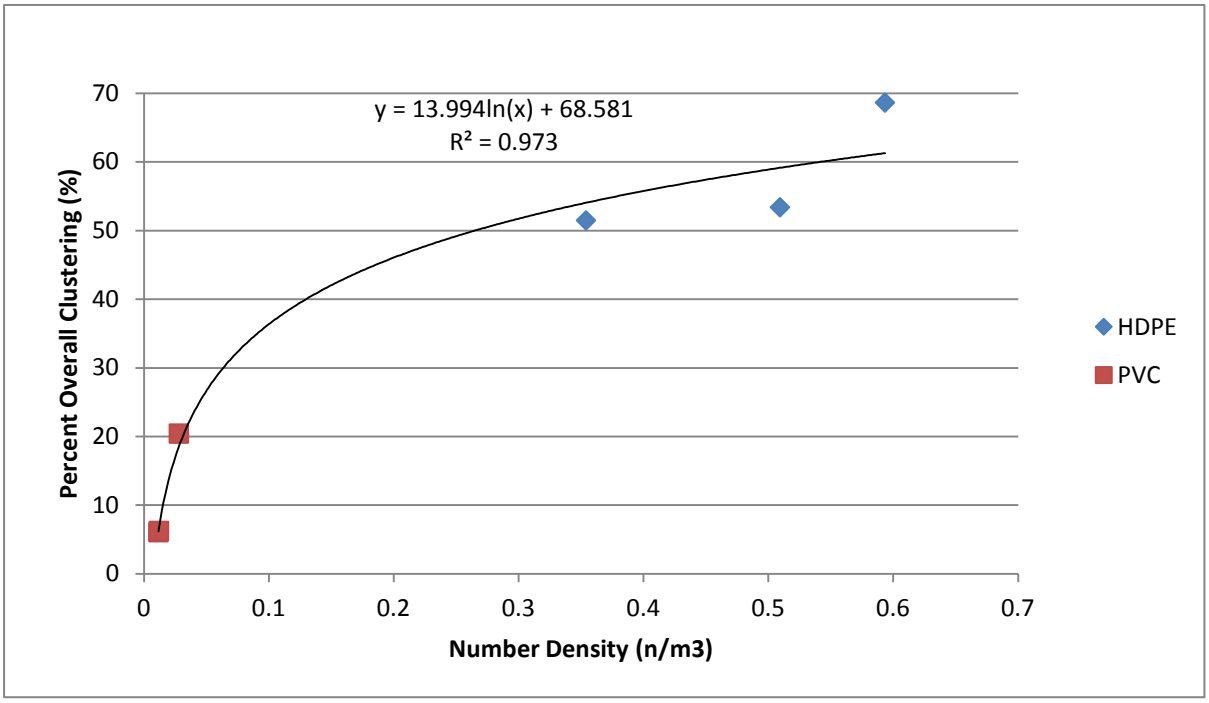

Figure 5-11: Number density vs. overall clustering (with Logarithmic fit)

Please Note: two data points for PVC are lying atop each other resulting in only two data points for PVC being displayed on the graph as opposed to the three data points for HDPE thus no data has been omitted.

The results of this analysis indicate that clustering in HDPE and PVC may lie on the same trend line (in terms of clustering expressed as a function of number density of the absorbed methanol) and therefore, the overall clustering may be directly related to the number density of the absorbed methanol and not, strictly speaking, to temperature, the amount of methanol absorbed, or even the nature of the polymer itself. What can instead be inferred is that the polymer indirectly affects the clustering of methanol by altering the free volume for which the methanol can insert itself during absorption. This would be dependent on the nature of the polymer and its behaviour in terms of how the chains arrange themselves such that spaces are created between chains to provide regions into which methanol molecules are able to move. These spaces can dictate the amount of clustering that may be possible. Figure 5-11 also indicates that once the number density is increased beyond a certain point, the overall clustering is not greatly affected. Consequently, it is difficult to ascertain whether chlorine itself has a direct influence on the clustering as both HDPE and PVC display a very similar

trend in this particular analysis. As stated previously, the effect of the chlorine atoms on the PVC chains may instead be indirect, as the chlorine-chlorine interactions between PVC polymer chains may alter the space in between molecules as compared to the case for HDPE.

It has been shown that absorption is not directly dependent on the atoms constituting the polymers but rather on the spaces between the polymer chain and that number density decreases with temperature. It can then be seen that for a fixed volume of polymer there is less absorbed methanol. This study was not concerned with time domain properties and therefore information about the kinetics of absorption cannot be obtained. This is because absorption is an equilibrium property and Monte Carlo methods are more suited than molecular dynamics to studying equilibrium properties. Due to the decrease in the amount of absorption with an increase in temperature there seems to be adsorption rather than absorption occurring.

The results above represent equilibrium properties which essentially show the methanol-polymer systems at equilibrium. With regards to steady state equilibrium properties, the graph does not provide an indication of how long in terms of time it takes to reach equilibrium but only how long equilibrium is reached in terms of configurations. Steady state does not necessarily describe the dynamic behaviour of the system and only represents the system at equilibrium. Monte Carlo simulations conducted only considered energetic changes and not time-based changes thus only energetic perturbations were considered from the steady state using this approach.

A variable pressure isothermal apparatus would be required to experimentally determine adsorption isotherms because a pure methanol phase and varying pressure while temperature remains constant is required to fit data to an isotherm model. Such an apparatus may also be used to undertake time domain measurements, which may be coupled with molecular dynamics simulations and the results of the present study for a more thorough analysis of this behaviour.

5.7 Swelling

Swelling is a usual phenomenon of interaction of a polymer with a solvent. Swelling results in an increase in the volume of the polymer. Swelling in polymers will reflect how applicable the solvent is for the polymer under consideration. The extent of swelling can be determined from the following formula:

$$\text{Percent Swelling (\%)} = \left| \frac{\left(\frac{1}{\rho}\right)absorbed - \left(\frac{1}{\rho}\right)pure}{\left(\frac{1}{\rho}\right)pure} \right| \times 100 \qquad \text{(Eq. 23)}$$

Where: $\rho_{absorebed}$ is the density of polymer after absorption (in g/ml), and

ρ_{pure} is the density of polymer before absorption (in g/ml)

Swelling was analysed because it can reduce the tensile strengths of polymers, since the polymer molecules interact less strongly if they are further apart.

As mentioned earlier, there was a higher absorption of methanol into PVC than HDPE however, less clustering was observed in PVC. It is possible that the methanol molecules cause the PVC polymer matrix to swell more than that of HDPE even though the cluster formation is lower. Swelling is related to clustering in that swelling is the reciprocal of density,and more clustering may imply a lower density polymer matrix due the presence of more free volume for cluster formation. Closer analysis showed that at 25 ^{o}C the density of PVC was at 0.03 g/ml and in HDPE the density was at 0.4 g/ml. This shows that the PVC polymer matrix was nearly doubled in size by the uptake of methanol while the HDPE polymer matrix was only 0.5 times bigger in size. As seen in the work of Johansson, Bolton and Ahlström (2008), where water molecules penetrated the polyethylene matrix forming “water trees” and induced breakdown of the material, clustering is known to diminish the structural integrity of polymers. Clustering, however, should be considered in conjunction with swelling because clusters may of course force polymer molecules apart, however, the results from this study show that this may not necessarily always be the case since PVC has more swelling while also having less clustering. This observation may be considered in conjunction with the previously stated analysis on the dependence of clustering on number

density of the absorbed methanol. The results of these different analyses suggest that there may be a highly nuanced relationship between cluster formation, swelling, and free volume in the polymer phase.

5.8 Effects of Changes in Cluster Radius

As a further means of analysis, the cluster radius for HDPE and PVC were increased and decreased to analyse the effect the cluster radius has on the amount of clustering in each type of polymer. In each case, the cluster radius was increased or decreased by 10%.

5.8.1 Decreased Cluster Radius

The decrease in cluster radius resulted in less clustering of all types in HDPE. Linear clusters still dominated over the cyclic and branched clusters but were still at least 1% lower in all cases in comparison to the original cluster radius.

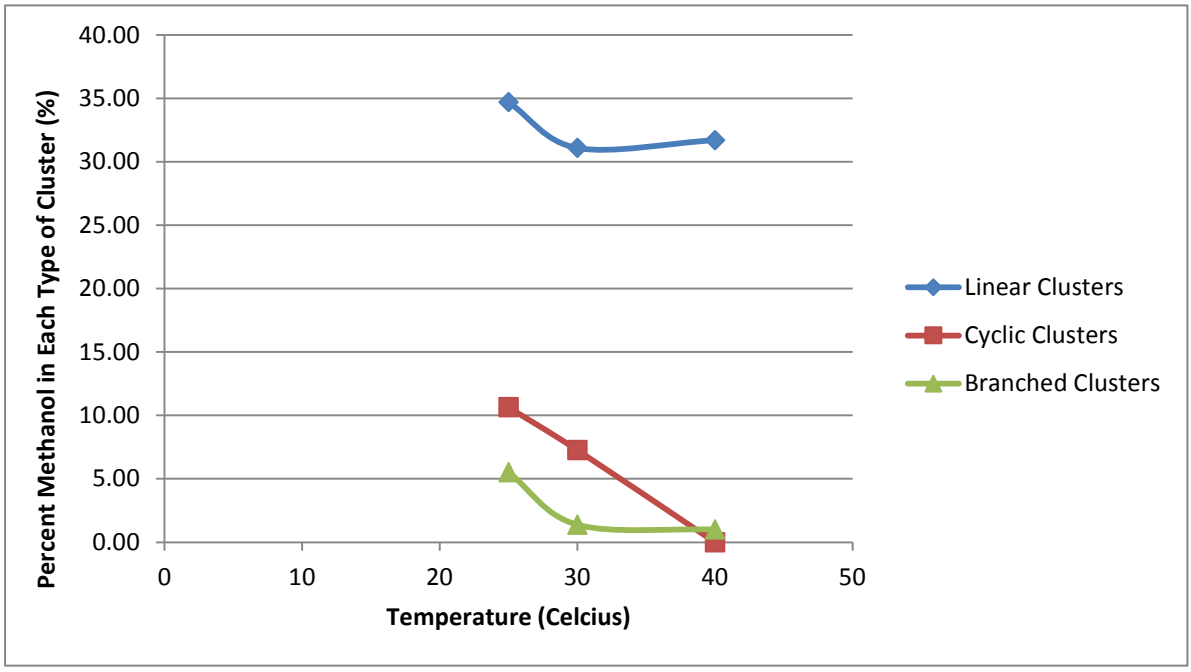

Figure 5-12: Different types of clustering in HDPE for a decreased cluster radius

A significant decrease in cyclic and branched clusters was seen where cyclic clusters were reduced to 0% at 40 ^{o}C. This suggests that in the cyclic clusters, the methanol molecules were only just part of the clusters, and were actually further away from each other than when

methanol molecules are found in linear configurations. When comparing these results to those obtained for the original cluster radius, there is a large difference. The original cluster radius resulted in decreases of 16% for cyclic clusters and 1% for branched clusters with an increase in temperature whereas a reduced cluster radius saw cyclic and branched clustering being reduced to zero with an increase in temperature.

When observing the effect of decreased cluster radius on PVC, it can be seen that the appearance of cyclic and branched clusters are approximately zero and therefore negligible. Linear clusters once again dominate but also decrease significantly to 4%. The type 1 cluster topology, which corresponds to methanol dimers, is the main type of clustering of the linear clusters.

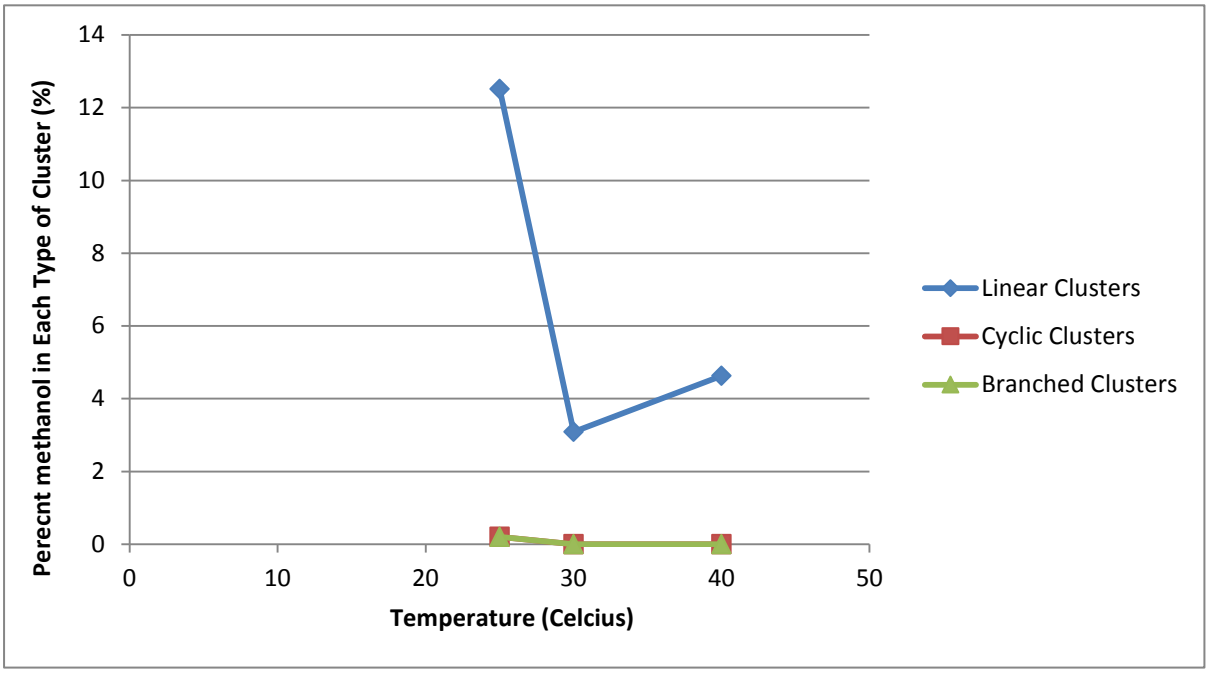

Figure 5-13: Different types of clustering in PVC for a decreased cluster radius

The comparison of overall clustering between HDPE and PVC shows that HDPE displays a much higher rate of clustering than PVC but in both cases the amount of clustering is still less than that achieved when using the original cluster radius. The original cluster radius resulted in an overall decrease of 17% for HDPE and 14% for PVC but when the cluster radius was decreased, the overall reduction for HDPE fell to 12% and to 9% for PVC.

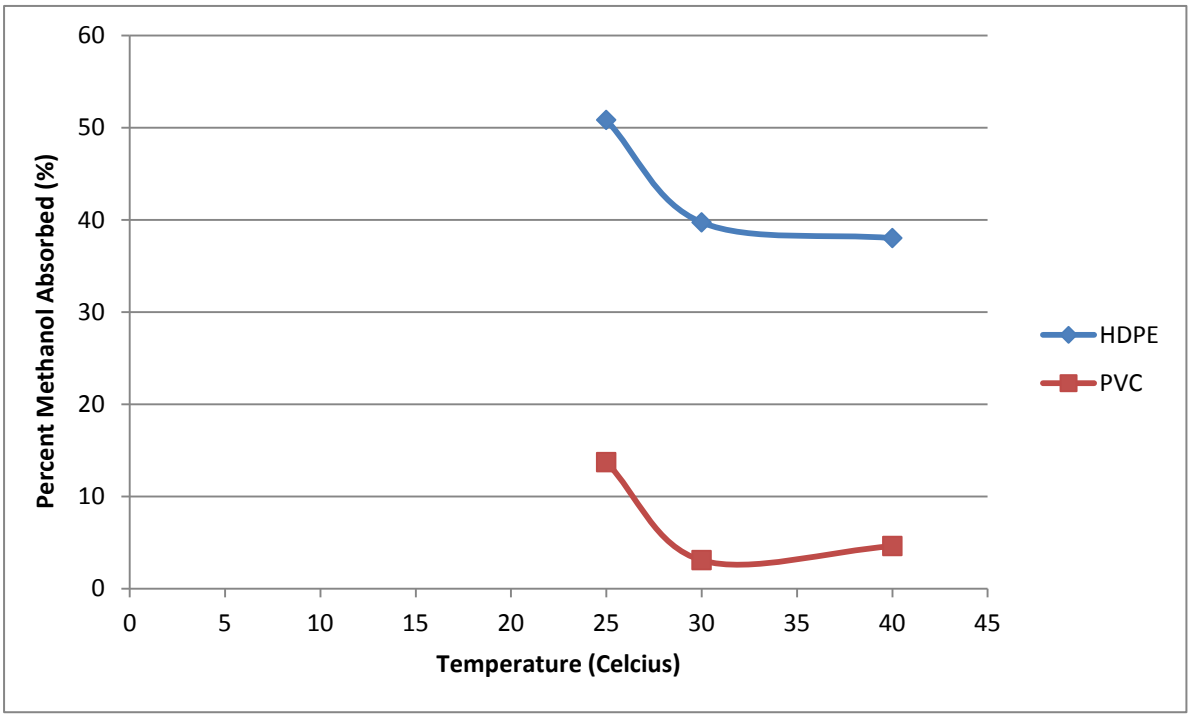

Figure 5-14: Comparison of overall clustering between HDPE and PVC for a decreased cluster radius

5.8.2 Increased Cluster Radius

In addition to a decrease in the cluster radius, an increase in the cluster rations was considered. It can be noted again that the cluster definition does not influence the amount of methanol absorbed, only the detected occurrence of methanol clusters once the methanol molecules are already absorbed. All cluster types showed a decreasing trend in clustering with increasing temperature, with cyclic clusters showing a very slight increase that can be considered negligible.

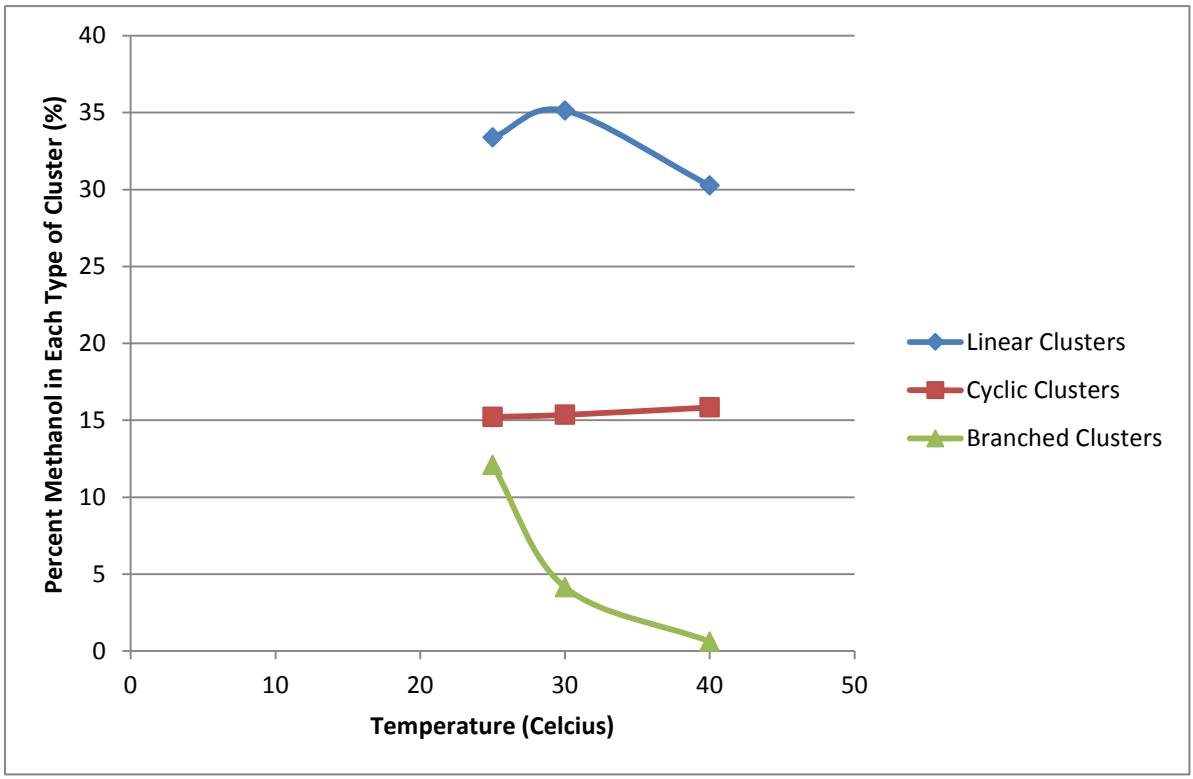

Figure 5-15: Different types of clustering in HDPE for an increased cluster radius

Decreasing clustering trends with increases in temperature were also observed with an increase in cluster radius for PVC. The major portion of clusters constituted linear clusters with type 1 topology being the dominant cluster type. Again, cyclic and branched clustering showed very little contribution to clustering as a whole and decreased to negligible amounts. The trend obtained by an increase in cluster radius for PVC parallels that of the trend displayed by the original cluster radius as the variation in total absorbed amounts for each type of clustering vary by 1 -2 %.

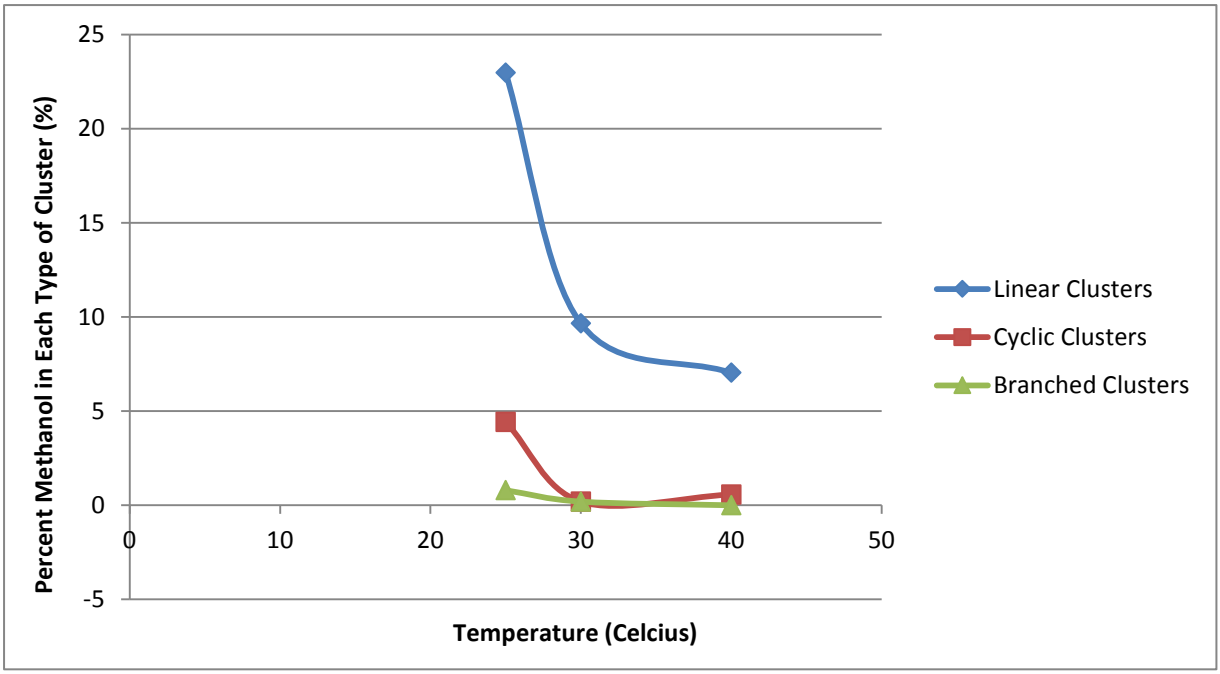

Figure 5-16: Different types of clustering in PVC for an increased cluster radius

The overall clustering as a result of an increase in cluster radius shows that HDPE has greater clustering than PVC but the total overall clustering achieved is higher in both polymers when the cluster radius was increased, with an increase in temperature, as opposed to when it was decreased. This trend is also observed when comparing the results from an increased cluster radius to the original cluster radius.

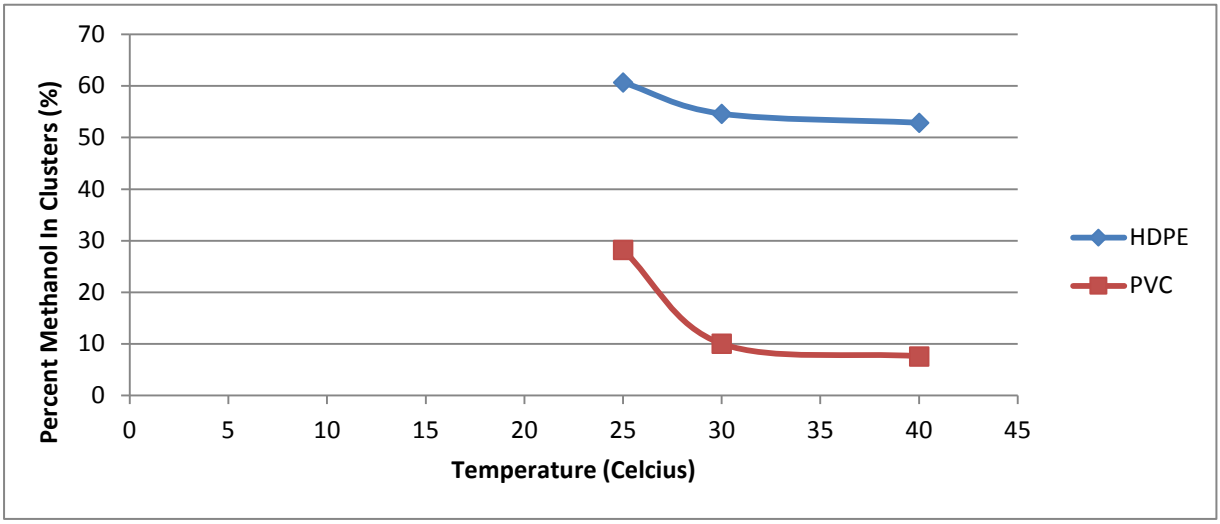

Figure 5-17: Comparison of overall clustering between HDPE and PVC for an increased cluster radius

It can be seen that the effect of increasing and decreasing the cluster radius does not have a major effect on the types of clustering (i.e. linear, cyclic or branched) achieved in that no changes in the variation of cluster types are caused since linear clusters predominate in both cases. Of those linear clusters, the type 1 cluster topology, which are dimers, are greater in presence. Figure 5-19 below illustrates that as temperature increases, the prevalence of dimers in both HDPE and PVC increase. This figure represents data from the original cluster radius.

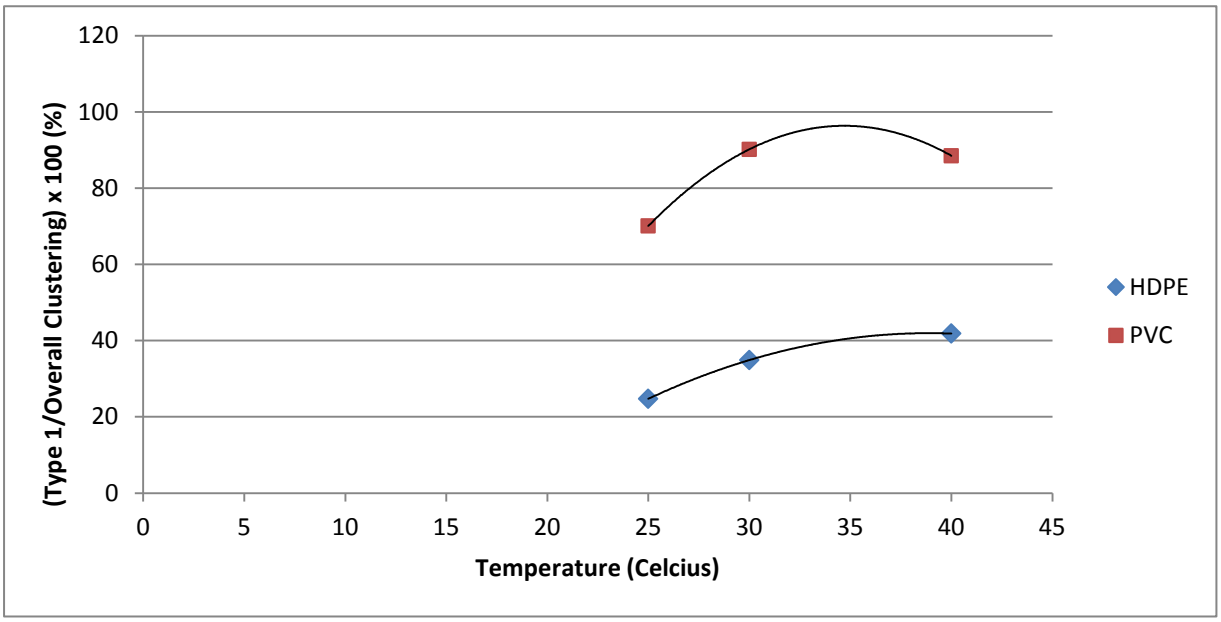

Figure 5-18: Cluster size analysis for type 1 topology

HDPE and PVC displayed a decrease in clustering with both an increased and decreased cluster radius. Similar trends for PVC were observed when the cluster radius was both increased and decreased since in both cases the cyclic and branched clustering was reduced to negligible amounts and linear clusters decreased to below 10% with an increase in temperature. Overall, HDPE still displays higher clustering with an increase in temperature regardless of the change (either increase or decrease) in the cluster radius. These changes were tested in order to gain insight on what degree of difference the cluster definition can make in terms of absorption and the clustering thereof. An increase in the cluster radius showed a small variation in the amount of overall clustering when compared to the original cluster radius, however, a decrease in the cluster radius resulted in a noticeable decrease in

the amount of overall clustering with an increase in temperature. The trends of HDPE and PVC in all cases (i.e. original cluster radius, decreased radius and increased radius) remains consistent regardless of the cluster definition, showing the cluster analysis was robust in terms of how the polymers perform relative to one another.This test was done in order to verify the cluster definition used as the cluster definition can have a great impact on how clustering is identified.

A study by Wedekind and Reguera (2007) showed that the ability of the Stillinger cluster definition to accurately identify physically relevant clusters was rather overestimated. To reiterate, clustering is the process of examining a collection of 'points' and then grouping these 'points' into clusters according to some specified distance measure. The intended aim is that the 'points' that are considered to be in the same cluster have a small distance from one another while 'points' in different clusters are at a larger distance from each other. They compared the Stillinger cluster definition with the ten Wolde and Frenkel (TWF) definition. They found that clusters sizes were always larger when described by the Stillinger definition than when described by the TWF definition, and depending on the cohesion parameters, the resulting error can at times be as large as a factor of 2. This limitation of the Stillinger criterion should be considered when examining the results of the present study, although it is expected that this would not change the trends observed, both in terms of temperature-dependence and the differences between the polymers.

CHAPTER 6: CONCLUSIONS

"The only thing I know for sure is that I know nothing at all." __ Socrates

The 20 carbon chain length polymers displayed a closer fit to experimental density than polymer chains of 50 carbon atoms and were therefore the chain size used in the simulations.

Experimental tests showed a decrease in absorption with an increase in clustering which suggests adsorption rather than absorption is occurring.

Experimental tests and simulations displayed the same decreasing trend in absorption with an increase in temperature. Simulations also showed that an increase in temperature resulted in a decrease in the amount of clustering in both HDPE and PVC. The greater uptake of methanol as seen in the simulations compared to the experimental tests are attributed to the of methanol phase of the United Force Field which overestimated the density of methanol in the fluid phase. Simulation results were adjusted for high and low crystallinity to account for the crystalline portions that are existent in real polymers

Cluster analysis showed that an increase in temperature resulted in a decrease in clustering in both HDPE and PVC with the degree of decrease being larger in PVC than HDPE. This suggested that chlorine atoms interfere with the absorption and clustering process. Overall, the decrease in absorption and clustering was more prominent in PVC than HDPE, with an increase in temperature. The overall clustering may be directly related to the number density of the absorbed methanol and not, strictly speaking, to temperature, the amounts of methanol absorbed, or even the nature of the polymer itself as the polymer indirectly affects the clustering of methanol by altering the free volume for which the methanol can insert itself during absorption.

Cluster topology type 1, which are dimers, were the most prevalent in the linear clusters in both HDPE and PVC. Increasing the temperature had a greater effect on reducing the amount of cyclic and branched clusters formed in PVC than HDPE, reducing these clusters to zero.

Swelling was considered in conjunction with clustering because it also contributes to the degradation of the strength of the polymer by forcing the molecules apart. PVC displayed a higher rate of swelling than HDPE despite having a lower rate of clustering. It can be concluded that clustering and swelling do not always have a direct relationship since PVC had a higher degree of swelling but a lower rate of clustering that HDPE.

The effect of changes in the cluster radius was studied to determine the effect the cluster definition has on the amount of clustering obtained. Decreasing the cluster radius resulted in a decrease in clustering in both PVC and HDPE although the overall clustering was still higher in HDPE but in both polymers the decrease in clustering was more than that of the original cluster radius. The trend displayed by both HDPE and PVC in all cases were relatively constant. Due to this trend it can be concluded that the cluster analysis was fairly robust in how the polymers perform relative to each other.

The overall clustering as a result of an increase in cluster radius showed that HDPE had greater clustering than PVC but the total overall clustering achieved is higher in both polymers when the cluster radius was increased, with an increase in temperature, as opposed to when it was decreased. This trend is also observed when comparing the results from an increased cluster radius to the original cluster radius.

CHAPTER 7: RECOMMENDATIONS

“Never replicate a successful experiment.” __Fett’s Law

Measurements should be repeated at different pressures to build up adsorption isotherm data to determine the type of adsorption occurring.

Nitrogen should be used to determine the B.E.T surface area to obtain a more detailed view of adsorption.

Simulations can be performed to complement these adsorption measurements.

An ab-initio study can be done to determine whether a particular dimer configuration is being favoured by the cluster definition as used in this study.

The cluster analysis routine can also be used to examine the behaviour of solvents such as water or alcohols with complex organic molecules like amino acids.

REFERENCES

"Books serve to show a man that those original thoughts of his aren't very new at all."

__ Abraham Lincoln

- Atkins, P.B. 1990. Physical Chemistry. Oxford, UK: Oxford University Press.
- Allen, M. P. and Tildesley, D. J. 1987. Computer Simulation of Liquids. 2nd Edition, Oxford: Claredon Press.
- Bolton, K., Johansson, E. L., Jönsson, L. and Ahlström, P. 2009. Simulation of Water Clusters in Vapour, Alkanes and Polyethylenes. *Molecular Simulation*, 35: 10-11, 888-896
- Börjesson, A., Erdtman, A., Ahlström, P., Berlin, M., Andersson, T. and Bolton K. 2013. Molecular Modelling of Oxygen and Water Permeation in Polyethylene. *Polymer*, 54(12): 2988- 2998
- Dlubek, G., Saarinen, K. and Fretwell, H. M. 1997. The Temperature Dependence of the Local Free Volume in Polyethylene and Polytetrafluoroethylene: A Positron Lifetime Study. *Journal of Polymer Science: Part B:Polymer Physics*, 36: 1513
- Freire, M. G., Carvalho, P. J.,Santos, L. M. N. B.F., Gomes, L.R. Marrucho, I. M and Coutinho, J. A. P. 2009. Solubility of Water in Fluorocarbons: Experimental and COSMO-RS Prediction Results. *Journal of Chemical Thermodynamics*, 42: 213-219
- Frenkel, D. and Smit, B. 2001. Understanding Molecular Simulation: From Algorithms to Applications. 2nd Edition, San Diego, California: Academic Press.
- Fuchs, A., Boutin, A. and Rousseau, B. 1998. Molecular Simulations as a Tool for Predicting Phase Equilibria and Transport Properties of Fluids. *Revue De L'Institut Fransçais Du Pètrole,*53(3)
- Gubbins, J. W. 1993. Applications of Molecular Simulation Fluid Phase Equilibria. 83:1-14
- Hodge, R. M., Edward, G. H. and Simon, G. P. 1996. Water Absorption and States of Water in Semicrystalline Poly (vinyl alcohol) Films. *Polymer*, 37 (8): 1371- 1376

- Irvine, M. and Marzani, N. 2005. Two Postulates of Statistical Mechanics and the Microscopic Definition of Entropy. Fundamentals of Material Science (3.012). Department of Chemical Engineering. Massachusetts Institute of Technology.
- Johansson, E. L. 2007. Simulations of Water Clustering in Vapour, Hydrocarbons and Polymers. Thesis for the Degree of Doctor of Philosophy, Chamlers University of Technology: Göteborg, Sweden
- Johansson, E. L., Bolton, K. and Ahlström, P. 2005. Simulation of Water Vapour Clusters in Equilibrium with Liquid Water. *Computer Physics Communications*, 169: 54-56
- Johansson, E. L., Bolton, K. and Ahlström, P. 2008. Molecular Simulation of the Effect of Ionic Impurities and External Electric Fields on Rod-Like Water Clusters in Polyethylene. *Polymer*, 49: 5357 - 5362
- Johansson, E. L., Bolton, K., Theodorou, D. N. and Ahlström, P. 2007. Monte Carlo Simulations of Equilibrium Solubilities and Structure of Water in n-Alkanes and Polyethylene. *Journal of Chemical Physics*, 126
- Lasich, M., Bhownath, R., Naidoo, P., Ramjugernath, D. and Moodley, T. 2011. Liquid-Liquid Equilibria of Methanol, Ethanol and Propan-2-ol with Water and Dodecane. *Journal of Chemical and Engineering Data*, 56: 4139 -4146
- Lasich, M., Johansson, E. L. and Ramjugernath, D. 2011. Water Solubility in Polytetrafluoroethylene by Molecular Simulation. Thermodynamics Conference, Athens, Greece
- Lasich, M., Johansson, E. L. and Ramjugernath, D. 2013. Monte Carlo Simulations of Water Solubility and Structuring in Poly(difluoromethylene). *Molecular Simulation*, 39: 367 - 384
- Lennard-Jones, J. E. 1931. “Cohesion” Proceedings of the Physical Society, 43: 461
- Lennert, T. J., Hendra, P. J., Everall, N. and Clayden, N. J. 1997. Comparative Quantitative Study on the Crystallinity of Poly(tetrafluoroethylene) including Raman, Infra-red and F^{19} Nuclear Magnetic Resonance Spectroscopy. *Polymer*, 38(7): 1521-1535
- Li, T., Kildsig, D. O. and Park, K. 1997. Computer Simulation of Molecular Diffusion in Amorphous Polymers. *Journal of Controlled Release*, 48: 57-66

- Metropolis, N.,Rosenbluth, W. A., Rosenbluth, M. N., and Teller, A. H. 1953. Equation of State Calculations by Fast Computing Machines. *Journal of Chemical Physics*, 21(6): 1087-1092
- Metropolis, N. 1987. The Beginning of the Monte Carlo Method. Los Alamos Science Special: 125-130.
- Mingxue, G., Wenchuan, W. and Huanzhang, L. 1992. Gibbs Ensemble Monte Carlo Simulation of Vapour-Liquid Equilibria for Simple Fluids. *Journal of Chemical Industry and Engineering (China)*, 7(2)
- Moodley, S. 2008. Molecular Simulation of Vapour –Liquid-Liquid Equilibrium. Thesis for the Degree of Master of Science in Engineering, University of Kwa-Zulu Natal, Durban: South Africa
- Nguyen, Q. T., Favre, E., Ping, Z. H. and Nèel, J. 1995. Clustering of Solvents in Membranes and its Influence on Membrane Transport Properties. *Journal of Membrane Science*, 113: 137-150.
- Pal, S., Weiss, H., Keller, H. and Müller-Plathe, F. 2005. The Hydrophobicity of Nanostructured Alkane and Perfluoroalkane Surfaces: A Comparison by Molecular Dynamics Simulation. *Phys. Chem. Chem. Phys*, 7: 3191-3196
- Pangiotopoulos, A. Z. 1987. Direct Determination of Phase Coexistence Properties of Fluids by Monte Carlo Simulation in a New Ensemble. *Molecular Physics*, 61: 813
- Pant, P. V. K. and Boyd, R. H. 1993. Molecular Dynamics Simulation of Diffusion of Small Penetrants in Polymers. *Macromolecules*, 26
- Rae, P. J., and Dattelbaum,D. M. 2004. The Properties of Poly(tetrafluoroethylene) (PTFE) in Compression. *Polymer*, 45: 7615-7625
- Rahmati, M., Modarress, H., and Gooya, R. 2012. Molecular Simulation Study of Polyurethane Membranes. *Journal of Polymer Science*, 53: 1939-1950
- Rappè, A. K., Casewit, C. J., Colwell, K. S., Goddard, W. A., and Skiff, W. M. 1992. UFF, A Full Periodic Table Force Field for Molecular Mechanics and Molecular Dynamics Simulations. *Journal of American Chemical Society*, 114(25): 10024-10035
- Rosenbluth, M. N., and Rosenbluth, A. W. 1955. Monte Carlo Calculation of the Average Extension of Molecular Chains. *Journal of Chemical Physics*, 97(2): 356
- Sarassin, F., Memari, P., Klopffer, M. H., Lachet, V., TaravekCondat, C., Rousseau, C., and Espuche, E. 2015. Influence of High Pressures on CH_4, CO_2 and H_2S Solubility in Polyethylene: Experimental and Molecular Simulation Approaches for

Pure Gas and Gas Mixtures. Modelling of the Sorption Isotherms. *Journal of Membrane Science*, 490: 380-388

- Seo, G. Y., Kum, G. H., and Seaton, N. A. 2001. Monte Carlo Simulation of Transport Diffusion in Nanoporous Carbon Membranes. *Journal of Membrane Science*, 195: 65-73
- Siepmann, J. I. 1990. A Method for the Direct Calculation of Chemical Potentials for Dense Chain Molecules. *The Journal of Chemical Physics*, 97: 2817
- Smith, J. M., Van Ness, H. C., and Abbott, M. M. 2005. Introduction to Chemical Engineering Thermodynamics. 7th Edition, McGraw-Hill: New York
- Sterling, T. 2002. Beowulf Cluster Computing with Linux. England: The MIT Press.
- Stillenger, F. H. 1963. Rigorous Basis of the Frenkel-Band Theory of Association Equlibrium. *The Journal of Chemical Physics*, 38: 1486
- Tamai, Y. 1994. Molecular Simulation of Permeation of Small Penetrants through Membranes. 1. Diffusion Coefficients, 27(16): 4498-4508
- Talu, O. and Myers, A, L. 2001. Reference Potentials For Adsorption of Helium, Argon, Methane and Krypton in High-Silica Zeolites. *Colloids and Surfaces A: Physiochemical and Engineering Aspects*, 187-188: 83-93
- Tsonopoulos, C. 1999. Thermodynamic Analysis of the Mutual Solubilities of Normal Alkanes and Water. *Fluid Phase Equilibria*, 156: 21
- Wedekind, J and Reguera, D. 2007. What is the Best Definition of a Liquid Cluster at the Molecular Scale.*The Journal of Chemical Physics*, 127: 154516-1 – 154516-6
- Woller, J. B. 1997. Determination of the Thermodynamic Properties of Fluids by Gibbs Ensemble Monte Carlo Computer Simulations. Thesis for the Degree of Master of Science in Chemistry, University of Nebraska: Lincoln, Nebraska

URL's

- Avogadro.cc/wiki/Main_Page (Accessed: 16 April 2016)
- Polymer.bu.edu/Wasser/Robert/work/node8.html (Accessed: 19 March 2016)
- http://towhee.sourceforge.net/ (Accessed: 14 May 2016)
- https://www.mathworks.com/ (Accessed: 3 August 2016)

APPENDIX A: EXPERIMENTAL RAW DATA

Polyvinylchloride (PVC)					
Temperature (^{0}C)	40				
		Weight Before (g)	Weight After (g)	Increase (g)	g Methanol/ 100g polymer
Sample	A	0,9848	0,9849	0,0001	0,010154346
	B	0,9852	0,9854	0,0002	0,020300447
	C	0,9951	0,9951	0	0
					0,010151598
Temperature (^{0}C)	30				
		Weight Before (g)	Weight After (g)	Increase (g)	g Methanol/ 100g polymer
Sample	A	0,9941	0,9947	0,0006	0,060356101
	B	1,0287	1,0287	0	0
	C	0,9644	0,9645	0,0001	0,010369141
					0,023575081
Temperature (^{0}C)	25				
		Weight Before (g)	Weight After (g)	Increase (g)	g Methanol/ 100g polymer
Sample	A	0,986	0,9863	0,0003	0,030425963
	B	1,0202	1,0208	0,0006	0,058811998
	C	1,0259	1,0261	0,0002	0,019495077
					0,036244346
High Density Polyethylene (HDPE)					
Temperature (^{0}C)	40				
		Weight Before (g)	Weight After (g)	Increase (g)	g Methanol/ 100g polymer
Sample	A	0,8322	0,8323	0,0001	0,012016342
	B	0,7171	0,7172	0,0001	0,013945056
	C	0,7897	0,7897	0,0000	0
					0,0086538
Temperature (^{0}C)	30				
		Weight Before (g)	Weight After (g)	Increase (g)	g Methanol/ 100g polymer
Sample	A	0,7607	0,7608	0,0001	0,013145787
	B	0,7493	0,7494	0,0001	0,013345789
	C	0,8064	0,8065	0,0001	0,012400794
					0,012964123
Temperature (^{0}C)	25				
		Weight Before (g)	Weight After (g)	Increase (g)	g Methanol/ 100g polymer
Sample	A	0,7309	0,7311	0,0002	0,027363524
	B	0,7842	0,7842	0	0
	C	0,8253	0,8255	0,0002	0,024233612
					0,017199045

APPENDIX B: WATER BATH CALIBRATION

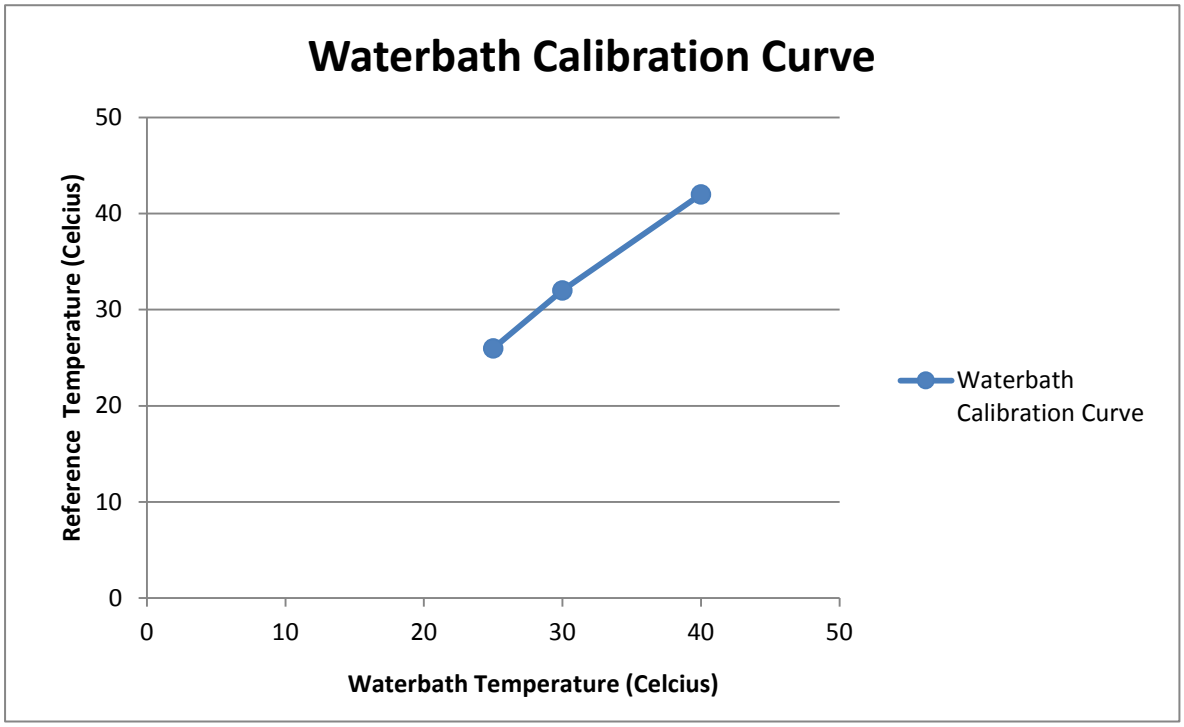

APPENDIX C: CONVERGENCE OF SIMULATED DATA

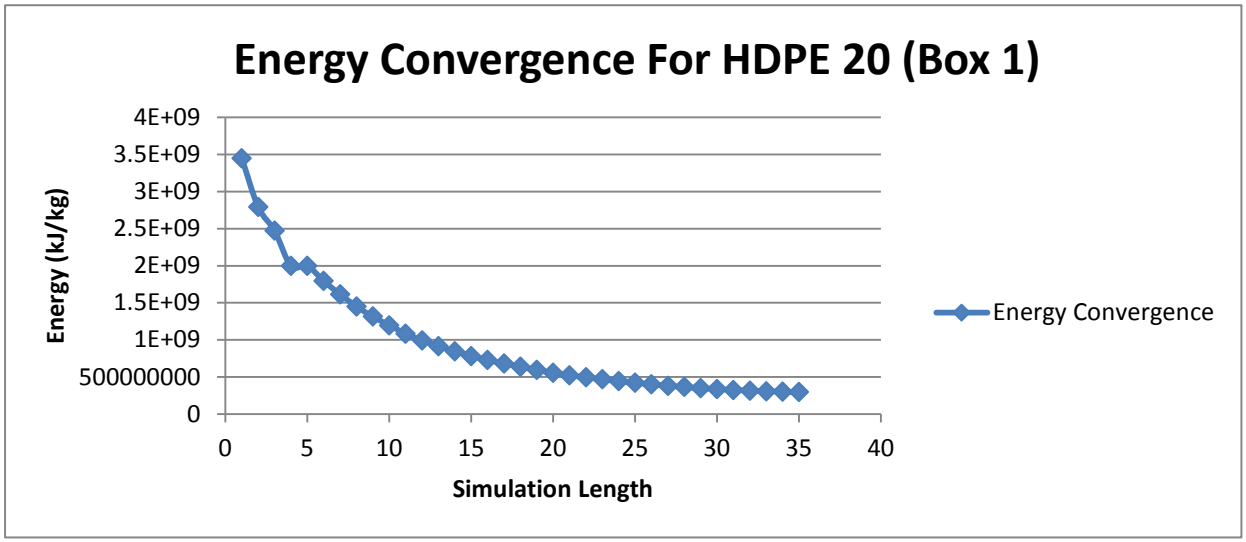

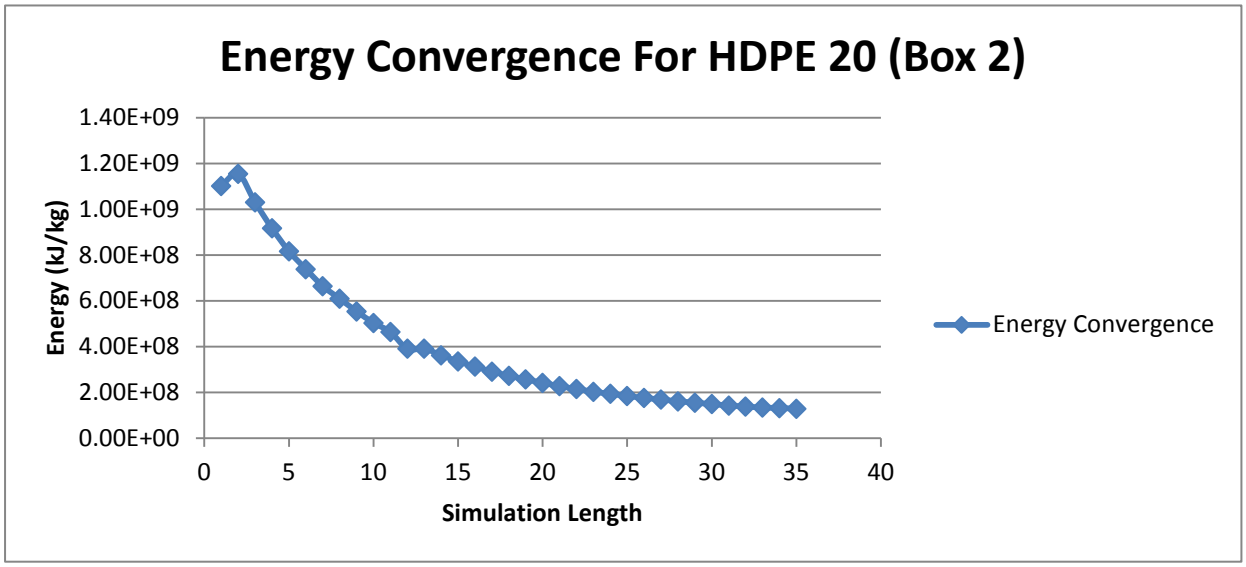

The above charts show the evolution of the energies of the simulation boxes as a function of the simulation length / number of cycles thus indicating that the energy converges to an asymptotic value.

APPENDIX D: MATLAB CODE FOR CLUSTER ANALYSIS

```
% CLUSTER ANALYSIS ROUTINE

% clearing the memory and display
clearall
clc

% note: it is assumed that box 1 is the polymer box and box 2 is the fluid
% box, however, it makes no difference to the actual calculation itself

% also note that steps should be stored in increments of 1000 moves/steps,
% and as a result, there cannot be 1000 molecules or more in the system,
% due to the approach used for searching through the towhee_movie file

% the distance criterion, in angstroms
criterion=1.5*3.207;

% total number of cycles in towhee_movie file
cycles=800;

% no. of atoms in polymer chain
npolymer=62;

% no. of atoms in gas molecule
ngas=6;

% Id number of gas species
gasID=20;

% our storage area
type1_store_polymer=[];
type2_store_polymer=[];
type3_store_polymer=[];
type4_store_polymer=[];
type5_store_polymer=[];
type6_store_polymer=[];
type7_store_polymer=[];

type1_store_fluid=[];
type2_store_fluid=[];
type3_store_fluid=[];
type4_store_fluid=[];
type5_store_fluid=[];
type6_store_fluid=[];
type7_store_fluid=[];
```

```
% now we have some repetitive calculations

% ------------------------------------------------------------------------

% read in the data
[val1 val2 val3 val4 val5] = textread('towhee_movie','%f %f %f %f %f');

% now to extract the coordinates of the methane molecules only
index=[];
for l=1:length(val1)
if val2(l)<1
if val1(l)<cycles
if val1(l)>30
if rem(val1(l),10)==0
if val1(l)~=0
index=[index; l];
end
end
end
end
end
end


for i = 1:length(index)

    y = index(i);

coords_polymer=[];
coords_fluid=[];


for
p=y+10:y+8+((val1(y+1)*npolymer+val2(y+1)*ngas+val1(y+5)*npolymer+val2(y+5)
*ngas+...
                    val1(y+1)+val2(y+1)+val1(y+5)+val2(y+5)))


%val4 is related to the box/phase. Storing the coordinates of the gas in
%the fluid phase.
if p+1<=numel(val5)

if val5(p+1)==gasID%matching the current selection with the fluid species

if val4(p-1)==1
%                         coords_polymer=[coords_polymer;...
%                             val1(p) val2(p) val3(p)];
coords_polymer=[coords_polymer;...

((val1(p)*12+val1(p+1)*16+val1(p+2)*1+val1(p+3)*1+val1(p+4)*1+val1(p+5)*1)/
32)
((val2(p)*12+val2(p+1)*16+val2(p+2)*1+val2(p+3)*1+val2(p+4)*1+val2(p+5)*1)/
32)
((val3(p)*12+val3(p+1)*16+val3(p+2)*1+val3(p+3)*1+val3(p+4)*1+val3(p+5)*1)/
32)];

elseif val4(p-1)==2
%coords_fluid=[coords_fluid;...
```

```
%val1(p) val2(p) val3(p)];
coords_fluid=[coords_fluid;...

((val1(p)*12+val1(p+1)*16+val1(p+2)*1+val1(p+3)*1+val1(p+4)*1+val1(p+5)*1)/
32)
((val2(p)*12+val2(p+1)*16+val2(p+2)*1+val2(p+3)*1+val2(p+4)*1+val2(p+5)*1)/
32)
((val3(p)*12+val3(p+1)*16+val3(p+2)*1+val3(p+3)*1+val3(p+4)*1+val3(p+5)*1)/
32)];
end

end
end



end

% % %



connection_store={};

for k=1:size(coords_polymer,1)

connection_indices=[k];
for m=1:size(coords_polymer,1)
                        d1=sqrt((coords_polymer(k,1)-
coords_polymer(m,1))^2+...
                        (coords_polymer(k,2)-coords_polymer(m,2))^2+...
                        (coords_polymer(k,3)-coords_polymer(m,3))^2);

if d1<=criterion
if d1~= 0
connection_indices=[connection_indices;m];
end
end


end
connection_store=[connection_store;connection_indices];

end




                type1=0;
                type2=0;
                type3=0;
                type4=0;
                type5=0;
                type6=0;
                type7=0;

for r=1:length(connection_store)
```

```
vala=connection_store{r};
now={length(vala)};
forrr=r+1:length(connection_store)
valb=connection_store{rr};
if sum(intersect(vala,valb))>0
now=[now;length(valb)];
connection_store{r}=[];
end
end

                    check1=0;
                    check2=0;
forrrr=1:length(now)
                        check1=check1+sum(now{rrr});
                        check2_temp=max(now{rrr});
if check2_temp>check2
                            check2=check2_temp;
end
end

switch check1
case 4
                            type1=type1+1;
case 7
                            type2=type2+1;
case 9
                            type3=type3+1;
case 10
switch check2
case 3
                                    type4=type4+1;
case 4
                                    type6=type6+1;
end
case 12
switch check2
case 3
                                    type5=type5+1;
case 4
                                    type7=type7+1;
end
end
end

if size(coords_polymer,1)==0
                    type1_store_polymer=[type1_store_polymer];
                    type2_store_polymer=[type2_store_polymer];
                    type3_store_polymer=[type3_store_polymer];
                    type4_store_polymer=[type4_store_polymer];
                    type5_store_polymer=[type5_store_polymer];
                    type6_store_polymer=[type6_store_polymer];
                    type7_store_polymer=[type7_store_polymer];

else
                type1_store_polymer=[type1_store_polymer;...
                    2*type1/size(coords_polymer,1)*100];
                type2_store_polymer=[type2_store_polymer;...
                    3*type2/size(coords_polymer,1)*100];
                type3_store_polymer=[type3_store_polymer;...
                    3*type3/size(coords_polymer,1)*100];
```

```
                type4_store_polymer=[type4_store_polymer;...
                    4*type4/size(coords_polymer,1)*100];
                type5_store_polymer=[type5_store_polymer;...
                    4*type5/size(coords_polymer,1)*100];
                type6_store_polymer=[type6_store_polymer;...
                    4*type6/size(coords_polymer,1)*100];
                type7_store_polymer=[type7_store_polymer;...
                    4*type7/size(coords_polymer,1)*100];
end


% % %




connection_store={};

for k=1:size(coords_fluid,1)

connection_indices=[k];
for m=1:size(coords_fluid,1)
                        d1=sqrt((coords_fluid(k,1)-coords_fluid(m,1))^2+...
                        (coords_fluid(k,2)-coords_fluid(m,2))^2+...
                        (coords_fluid(k,3)-coords_fluid(m,3))^2);

if d1<=criterion
if d1~= 0
connection_indices=[connection_indices;m];
end
end


end
connection_store=[connection_store;connection_indices];

end




                type1=0;
                type2=0;
                type3=0;
                type4=0;
                type5=0;
                type6=0;
                type7=0;

for r=1:length(connection_store)
vala=connection_store{r};
now={length(vala)};
forrr=r+1:length(connection_store)
valb=connection_store{rr};
if sum(intersect(vala,valb))>0
now=[now;length(valb)];
connection_store{r}=[];
```

```
end
end

                    check1=0;
                    check2=0;
forrrr=1:length(now)
                        check1=check1+sum(now{rrr});
                        check2_temp=max(now{rrr});
if check2_temp>check2
                            check2=check2_temp;
end
end



switch check1
case 4
                            type1=type1+1;
case 7
                            type2=type2+1;
case 9
                            type3=type3+1;
case 10
switch check2
case 3
                                    type4=type4+1;
case 4
                                    type6=type6+1;
end
case 12
switch check2
case 3
                                    type5=type5+1;
case 4
                                    type7=type7+1;
end
end
end

if size(coords_fluid,1)==0
                    type1_store_fluid=[type1_store_fluid];
                    type2_store_fluid=[type2_store_fluid];
                    type3_store_fluid=[type3_store_fluid];
                    type4_store_fluid=[type4_store_fluid];
                    type5_store_fluid=[type5_store_fluid];
                    type6_store_fluid=[type6_store_fluid];
                    type7_store_fluid=[type7_store_fluid];
else

                type1_store_fluid=[type1_store_fluid;...
                    2*type1/size(coords_fluid,1)*100];
                type2_store_fluid=[type2_store_fluid;...
                    3*type2/size(coords_fluid,1)*100];
                type3_store_fluid=[type3_store_fluid;...
                    3*type3/size(coords_fluid,1)*100];
                type4_store_fluid=[type4_store_fluid;...
                    4*type4/size(coords_fluid,1)*100];
                type5_store_fluid=[type5_store_fluid;...
                    4*type5/size(coords_fluid,1)*100];
                type6_store_fluid=[type6_store_fluid;...
                    4*type6/size(coords_fluid,1)*100];
```

```
                type7_store_fluid=[type7_store_fluid;...
                    4*type7/size(coords_fluid,1)*100];
end

end



% ------------------------------------------------------------------------
% displaying our results
disp('first, the topology field guide:')
disp(' ')
disp('type 1:')
disp('o - o')
disp(' ')
disp('type 2:')
disp('o - o - o')
disp(' ')
disp('type 3:')
disp('  o  ')
disp(' / \ ')
disp('o - o')
disp(' ')
disp('type 4:')
disp('o - o - o - o')
disp(' ')
disp('type 5:')
disp('o - o')
disp('|   |')
disp('o - o')
disp(' ')
disp('type 6:')
disp('    o    ')
disp('    |    ')
disp('o - o - o')
disp(' ')
disp('type 7:')
disp('  o      ')
disp(' / \     ')
disp('o - o - o')
disp(' ')

% % %
disp('detailed breakdown of topologies...')
disp(' ')
disp('type 1 clustering in the absorbed phase:')
X = [num2str(mean(type1_store_polymer)),' +/- ',...
num2str(std(type1_store_polymer)),' %'];
disp(X)
disp(' ')
disp('type 2 clustering in the absorbed phase:')
X = [num2str(mean(type2_store_polymer)),' +/- ',...
num2str(std(type2_store_polymer)),' %'];
disp(X)
disp(' ')
disp('type 3 clustering in the absorbed phase:')
X = [num2str(mean(type3_store_polymer)),' +/- ',...
num2str(std(type3_store_polymer)),' %'];
disp(X)
disp(' ')
```

```
disp('type 4 clustering in the absorbed phase:')
X = [num2str(mean(type4_store_polymer)),' +/- ',...
num2str(std(type4_store_polymer)),' %'];
disp(X)
disp(' ')
disp('type 5 clustering in the absorbed phase:')
X = [num2str(mean(type5_store_polymer)),' +/- ',...
num2str(std(type5_store_polymer)),' %'];
disp(X)
disp(' ')
disp('type 6 clustering in the absorbed phase:')
X = [num2str(mean(type6_store_polymer)),' +/- ',...
num2str(std(type6_store_polymer)),' %'];
disp(X)
disp(' ')
disp('type 7 clustering in the absorbed phase:')
X = [num2str(mean(type7_store_polymer)),' +/- ',...
num2str(std(type7_store_polymer)),' %'];
disp(X)
disp(' ')

% % %

disp('type 1 clustering in the fluid phase:')
X = [num2str(mean(type1_store_fluid)),' +/- ',...
num2str(std(type1_store_fluid)),' %'];
disp(X)
disp(' ')
disp('type 2 clustering in the fluid phase:')
X = [num2str(mean(type2_store_fluid)),' +/- ',...
num2str(std(type2_store_fluid)),' %'];
disp(X)
disp(' ')
disp('type 3 clustering in the fluid phase:')
X = [num2str(mean(type3_store_fluid)),' +/- ',...
num2str(std(type3_store_fluid)),' %'];
disp(X)
disp(' ')
disp('type 4 clustering in the fluid phase:')
X = [num2str(mean(type4_store_fluid)),' +/- ',...
num2str(std(type4_store_fluid)),' %'];
disp(X)
disp(' ')
disp('type 5 clustering in the fluid phase:')
X = [num2str(mean(type5_store_fluid)),' +/- ',...
num2str(std(type5_store_fluid)),' %'];
disp(X)
disp(' ')
disp('type 6 clustering in the fluid phase:')
X = [num2str(mean(type6_store_fluid)),' +/- ',...
num2str(std(type6_store_fluid)),' %'];
disp(X)
disp(' ')
disp('type 7 clustering in the fluid phase:')
X = [num2str(mean(type7_store_fluid)),' +/- ',...
num2str(std(type7_store_fluid)),' %'];
disp(X)
disp(' ')

% % %
```

```
disp('overall clustering...')
disp(' ')


disp('overall clustering in the absorbed phase:')
X = [num2str(sum([mean(type1_store_polymer),mean(type2_store_polymer),...
mean(type3_store_polymer),mean(type4_store_polymer),...
mean(type5_store_polymer),mean(type6_store_polymer),...
mean(type7_store_polymer)])),' +/- ',...
num2str(mean([std(type1_store_polymer),std(type2_store_polymer),...
std(type3_store_polymer),std(type4_store_polymer),...
std(type5_store_polymer),std(type6_store_polymer),...
std(type7_store_polymer)])),' %'];
disp(X)
disp(' ')

disp('overall clustering in the fluid phase:')
X = [num2str(sum([mean(type1_store_fluid),mean(type2_store_fluid),...
mean(type3_store_fluid),mean(type4_store_fluid),...
mean(type5_store_fluid),mean(type6_store_fluid),...
mean(type7_store_fluid)])),' +/- ',...
num2str(mean([std(type1_store_fluid),std(type2_store_fluid),...
std(type3_store_fluid),std(type4_store_fluid),...
std(type5_store_fluid),std(type6_store_fluid),...
std(type7_store_fluid)])),' %'];
disp(X)
disp(' ')
```

APPENDIX E: INPUT FILE DATA

```
inputformat
'Towhee'
ensemble
'npt'
temperature
298.15d0
pressure
101.325d0
nmolty
1
nmolectyp
48
numboxes
2
stepstyle
'cycles'
nstep
20000
controlstyle
'equilibration'
potentialstyle
'internal'
ffnumber
1
ff_filename
/towheebase/ForceFields/towhee_ff_UFF
classical_potential
'UFF 12-6'
classical_mixrule
'Geometric'
lshift
.false.
ltailc
F
rmin
```

1.0d0
rcut
14.0d0
rcutin
10.0d0
electrostatic_form
'none'
linit
F
initboxtype
'dimensions'
initstyle
'template'
'full cmbc'
initlattice
'simple cubic'
'simple cubic'
initmol
48
200
inix iniy iniz
4 4 3
6 6 6
hmatrix
40.0d0 0.0d0 0.0d0
0.0d0 40.0d0 0.0d0
0.0d0 0.0d0 30.0d0
200.0d0 0.0d0 0.0d0
0.0d0 200.0d0 0.0d0
0.0d0 0.0d0 200.0d0
pmvol
0.002d0

Pmvlpr

1.0d0
rmvol

0.1d0
tavol

0.5d0

pm2boxcbswap
0.2d0

pm2cbswmt

1.0d0
pm2cbswpr
1.0d0

pmcb
0.4d0

pmcbmt
1.0d0
pmall
0.0d0

pmtracm

0.7d0

pmtcmt
1.0d0
rmtrac
0.5d0

tatrac

0.5d0

Pmrotate

1.0d0
pmromt
1.0d0
rmrot
0.05d0

Tarot

0.5d0
input_style
'basic connectivity map'
nunit
152

nmaxcbmc
12
lpdbnames
F
forcefield
'UFF'

```
charge_assignment
'manual'
unit ntype qqatom
1    'C_1'   0.0d0
vibration
4
2 21 22 23
improper torsion
0
unit ntype qqatom
2    'C_1'  0.0d0
vibration
4
1 3 24 25
improper torsion
0
unit ntype qqatom
3 'C_1' 0.0d0
vibration
4
2 4 26 27
improper torsion
0
unit ntype qqatom
4    'C_1'   0.0d0

vibration
4
3 5 28 29
improper torsion
0
unit ntype qqatom
5    'C_1'  0.0d0
vibration
4
4 6 30 31
improper torsion
0
unit ntype qqatom
6 'C_1' 0.0d0
vibration
4
5 7 32 33
```

```
improper torsion
0
unit ntype qqatom
7 'C_1' 0.0d0
vibration
4
6 8 34 35
improper torsion
0
unit ntype qqatom
8    'C_1'   0.0d0
vibration
4
9 7 36 37
improper torsion
0
unit ntype qqatom
9    'C_1'  0.0d0
vibration
4
8 10 38 39
improper torsion
0
unit ntype qqatom
10 'C_1' 0.0d0
vibration
4
9 11 40 41
improper torsion
0
unit ntype qqatom
11 C_1' 0.0d0
vibration
4
10 12 42 43
improper torsion
0
unit ntype qqatom
12 'C_1' 0.0d0
vibration
4
11 13 44 45
```

```
improper torsion
0
unit ntype qqatom
13    'C_1'   0.0d0
vibration
4
12 14 46 47
improper torsion
0
unit ntype qqatom
14    'C_1'  0.0d0
vibration
4
13 15 48 49
improper torsion
0
unit ntype qqatom
15 'C_1' 0.0d0
vibration
4
14 16 50 51
improper torsion
0
unit ntype qqatom
16 'C_1' 0.0d0
vibration
4
15 17 52 53
improper torsion
0
unit ntype qqatom
17 'C_1' 0.0d0
vibration
4
16 18 54 55
improper torsion
0
unit ntype qqatom
18 'C_1'   0.0d0
vibration
4
17 19 56 57
improper torsion
0
```

unit ntype qqatom
19 'C_1' 0.0d0
vibration
4
18 20 58 59
improper torsion
0
unit ntype qqatom
20 'C_1' 0.0d0
vibration
4
19 60 61 62
improper torsion
0
unit ntype qqatom
1 'H_1' 0.0d0
vibration
1
1
improper torsion

0
unit ntype qqatom

22 'H_1' 0.0d0
vibration
1
1
improper torsion
0
unit ntype qqatom
23 'H_1'   0.0d0
vibration
1
1
improper torsion
0
unit ntype qqatom
24 'H_1' 0.0d0
vibration
1
2
improper torsion
0
unit ntype qqatom
25 'H_1' 0.0d0

```
vibration
1
2
improper torsion
0
unit ntype qqatom
26 'H_1' 0.0d0
vibration
1
3
improper torsion
0
unit ntype qqatom
27 'H_1' 0.0d0
vibration
1
3
improper torsion
0
unit ntype qqatom
28 'H_1'   0.0d0
vibration
1
4
improper torsion
0
unit ntype qqatom
29 'H_1'  0.0d0
vibration
1
4
improper torsion
0
unit ntype qqatom
30 'H_1' 0.0d0
vibration
1
5
improper torsion
0
unit ntype qqatom
31 'H_1' 0.0d0
vibration
1
5
```

```
improper torsion
0
unit ntype qqatom
32 'H_1' 0.0d0
vibration
1
6
improper torsion
0
unit ntype qqatom

33 'H_1'   0.0d0
vibration
1
6
improper torsion
0
unit ntype qqatom
34 'H_1'  0.0d0
vibration
1
7
improper torsion
0
unit ntype qqatom
35 'H_1' 0.0d0
vibration
1
7
improper torsion
0
unit ntype qqatom
36 'H_1' 0.0d0
vibration
1
8
improper torsion
0
unit ntype qqatom
37 'H_1' 0.0d0
vibration
1
8
improper torsion
```

0
unit ntype qqatom
38 'H_1'   0.0d0
vibration
1
9
improper torsion

0
unit ntype qqatom
39 'H_1' 0.0d0
vibration
1
9
improper torsion
0
unit ntype qqatom
40 'H_1' 0.0d0
vibration
1
10
improper torsion
0
unit ntype qqatom
41 'H_1' 0.0d0
vibration
1
10
improper torsion
0
unit ntype qqatom
42 'H_1' 0.0d0
vibration
1
11
improper torsion
0
unit ntype qqatom
43 'H_1'   0.0d0
vibration
1
11
improper torsion
0
unit ntype qqatom

44 'H_1' 0.0d0
vibration
1
12
improper torsion
0
unit ntype qqatom
45 'H_1' 0.0d0
vibration
1
12
improper torsion
0
unit ntype qqatom
46 'H_1' 0.0d0
vibration
1
13
improper torsion
0
unit ntype qqatom
47 'H_1' 0.0d0
vibration
1
13
improper torsion
0
unit ntype qqatom
48 'H_1'   0.0d0
vibration
1
14
improper torsion
0
unit ntype qqatom
49 'H_1' 0.0d0
vibration
1
14
improper torsion
0
unit ntype qqatom
50 'H_1' 0.0d0
vibration

1
15

improper torsion
0
unit ntype qqatom
51 'H_1' 0.0d0
vibration
1
15
improper torsion
0
unit ntype qqatom
52 'H_1' 0.0d0
vibration
1
16
improper torsion
0

unit ntype qqatom
53 'H_1'   0.0d0
vibration
1
16
improper torsion
0
unit ntype qqatom
54 'H_1' 0.0d0
vibration
1
17
improper torsion
0
unit ntype qqatom
55 'H_1' 0.0d0
vibration
1
17
improper torsion
0
unit ntype qqatom
56 'H_1' 0.0d0
vibration
1
18

```
improper torsion
0
unit ntype qqatom
57 'H_1' 0.0d0
vibration
1
18
improper torsion
0
unit ntype qqatom
58 'H_1'   0.0d0
vibration
1
19
improper torsion
0
unit ntype qqatom
59 'H_1'  0.0d0
vibration
1
19
improper torsion
0
unit ntype qqatom
60 'H_1' 0.0d0
vibration
1
20
improper torsion
0
unit ntype qqatom
61 'H_1' 0.0d0
vibration
1
20
improper torsion
0
unit ntype qqatom
62 'H_1' 0.0d0
vibration
1
20
improper torsion
0
input_style
```

'basic connectivity map'
nunit

6
nmxcmbc
6
lpdbnames
F
forcefield
'UFF'
change_assignment
'manual'
unit ntype qqatom
1 'C_1' 0.0d0
vibration
4
2 4 5 6
improper torsion
0
unit ntype qqatom
2 'O_1' 0.0d0
vibration
2
1 3
improper torsion
0
unit ntype qqatom
3 'H_1' 0.0d0
vibration
1
2
improper torsion
0

unit ntype qqatom
4 'H_1' 0.0d0
vibration
1
unit ntype qqatom
5 'H_1' 0.0d0
vibration
1
1
improper torsion
0

unit ntype qqatom
6 'H_1' 0.0d0
vibration
1
1
improper torsion
0